RESULTS

hHGF in plasma and tissues. In the hindlimb receiving the adenoviral vector (Ad.CAG-HGF), hHGF levels peaked at 4.35 ± 0.03 ng/mg 3 days after injection; no hHGF was detected in the hindlimbs of LacZ-treated mice (Fig. 1*A*). Plasma hHGF also peaked 3 days after injection of Ad.CAG-HGF (3.25 ± 0.85 ng/ml), and significant levels were sustained for an additional 9 days thereafter (Fig. 1*B*). Myocardial hHGF levels showed a similar pattern (Fig. 1*C*).

Effects of hHGF gene delivery on cardiac function and pathology. All mice in each group remained alive 4 wk after doxorubicin administration. Echocardiography and cardiac catheterization showed that, compared with the saline-treated controls, mice receiving doxorubicin had significant deterioration of left ventricular (LV) functionality characterized by an enlargement of the LV cavity and decreased LV fractional shortening and $\pm dP/dt$ (Fig. 2). The delivery of the hHGF gene significantly attenuated the doxorubicin-induced impairment of cardiac function.

No significant difference was observed in the heart weight-to-body weight ratios among the groups (saline, 3.78 ± 0.01; doxorubicin with LacZ, 3.87 ± 0.01; and doxorubicin with hHGF, 3.71 ± 0.01 mg/g). On the other hand, an examination of transverse sections of hearts stained with hematoxylin-eosin revealed that the sizes of cardiomyocytes (expressed as the transverse diameters) from the group receiving doxorubicin plus LacZ were significantly smaller than those in the saline group (11.5 ± 0.22 vs. 13.8 ± 0.37 μm, $P < 0.05$) and that hHGF delivery exerted a significant protective effect against such doxorubicin-induced cardiomyocyte atrophy (transverse diameter, 13.4 ± 0.18 μm) (Fig. 3). Similarly, when we assessed myocardial fibrosis using Sirius red-stained sections, we found significantly greater fibrosis in the group receiving doxorubicin plus LacZ than in groups receiving saline (0.99 ± 0.05% vs. 0.55 ± 0.04%, $P < 0.05$) or doxorubicin plus hHGF (0.58 ± 0.04%) (Fig. 3). Myocardial capillary density, which we assessed based on Flk-1 immunostaining, was unaffected by either doxorubicin or hHGF treatment (Fig. 3). Immunohistochemical analysis also revealed that CD45-positive leukocyte infiltration did not differ among the groups (Fig. 3).

Degenerative changes within cardiomyocytes caused by doxorubicin were clearly evident under an electron microscope, which confirmed previously described findings in doxorubicin-induced cardiomyopathy (16, 30). These changes were characterized by myofibrillar derangement and disruption and by increases in the volume of subcellular organelles such as mitochondria (Fig. 3). These degenerative changes were significantly mitigated by hHGF gene transfer. No apoptotic cells were ever detected by electron microscopic observation of cardiac tissue from any of the groups.

TUNEL-positive cardiomyocytes were detected, though very rarely, and the incidence was not affected by either doxorubicin administration or hHGF gene transfer (saline, 0.04 ± 0.03%; doxorubicin plus LacZ, 0.06 ± 0.03%; and doxorubicin plus hHGF, 0.05 ± 0.04%). Consistent with that finding, the active (cleaved) form of caspase-3 was not detectable in hearts from any of the groups by Western blot analysis (data not shown). The absence of apoptotic cells in the present model confirms earlier studies (16, 17). In addition, proliferating cardiomyocytes, as indicated by the presence of Ki-67, were never detected (data not shown).

Expression of c-Met/HGF receptor. The HGF receptor has been identified as c-Met, the product of the c-Met proto-oncogene (5, 6). Western blot analysis revealed that the expression of the c-Met/HGF receptor was significantly down-regulated in doxorubicin-treated hearts but was greatly enhanced by hHGF gene transfer (Fig. 4*A*). Consistent with this

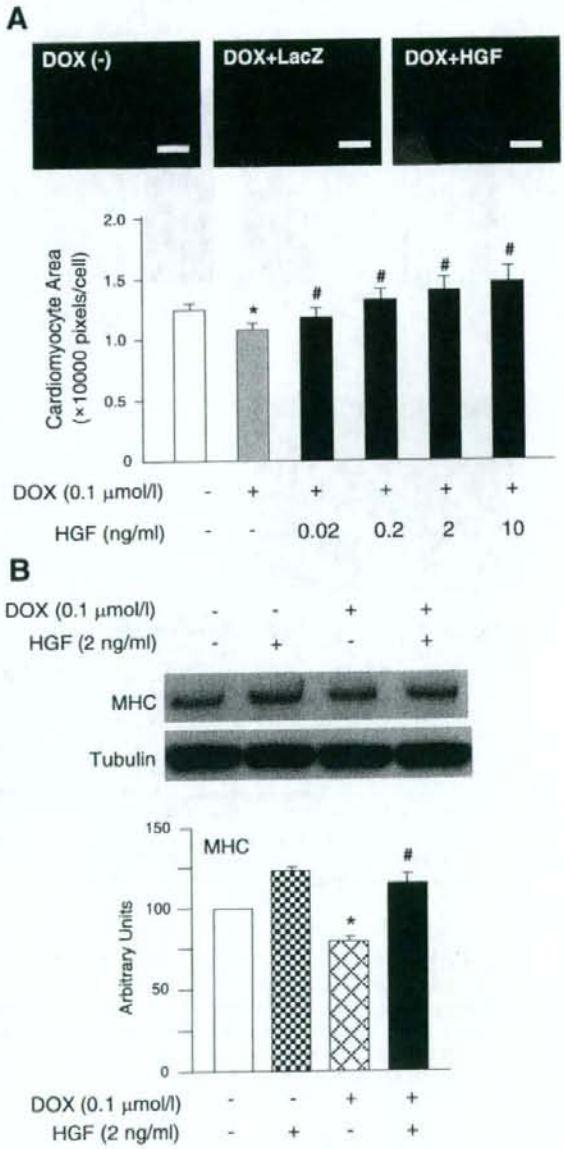

Fig. 6. In vitro experiments. *A*: confocal micrographs and a graph showing the atrophic degeneration of cardiomyocytes exposed to Dox and its prevention by recombinant hHGF. Bars, 10 μm. *$P < 0.05$ vs. sham group; #$P < 0.05$ vs. Dox + LacZ group. *B*: Western blot analysis of the effect of hHGF on the Dox-mediated reduction of MHC in cultured cardiomyocytes. *$P < 0.05$ vs. control group; #$P < 0.05$ vs. group treated with Dox alone.

finding, immunohistochemical analysis showed c-Met to be expressed on cardiomyocytes and to be more strongly expressed in hHGF-treated hearts (Fig. 4*B*).

Expression of GATA-4 and MHC. GATA-4 is a key transcriptional factor-regulating expression of sarcomeric proteins in the heart (22, 23). Myocardial levels of GATA-4 were significantly reduced by doxorubicin, confirming earlier reports (4). This reduction was significantly reversed by hHGF gene transfer (Fig. 5*A*). Likewise, the level of MHC was significantly reduced by doxorubicin, and this inhibitory effect was also significantly reversed by hHGF gene therapy (Fig. 5*A*).

Expression of TGF-β1 and cyclooxygenase-2. Doxorubicin had no significant effect on the expression of TGF-β1 or cyclooxygenase-2 in hearts 4 wk after administration, and neither was affected by hHGF gene transfer (Fig. 5*B*, data not shown).

In vitro effect of hHGF on cardiomyocytes. Doxorubicin exerted a significant atrophic/degenerative effect on cultured neonatal mouse cardiomyocytes, but this effect was largely reversed by an application of recombinant hHGF (Fig. 6*A*). hHGF affected the cardiomyocytes in a dose-dependent manner. Western blot analysis revealed that doxorubicin significantly reduced expression of MHC in cultured cardiomyocytes, but the expression was restored by the addition of hHGF to the cultures (Fig. 6*B*).

ERK activity. ERK/MAPK and phosphatidylinositol 3-kinase (PI3K)/Akt are known to be components of major signaling pathways downstream of c-Met/HGF receptor (9, 24). Neither doxorubicin-induced cardiomyopathy nor the effects of hHGF gene transfer was found to be related to the activation (phosphorylation) of Akt in the heart 4 wk after doxorubicin treatment (Fig. 7*A*). In contrast, ERK phosphorylation, and thus its activation, was markedly diminished by doxorubicin,

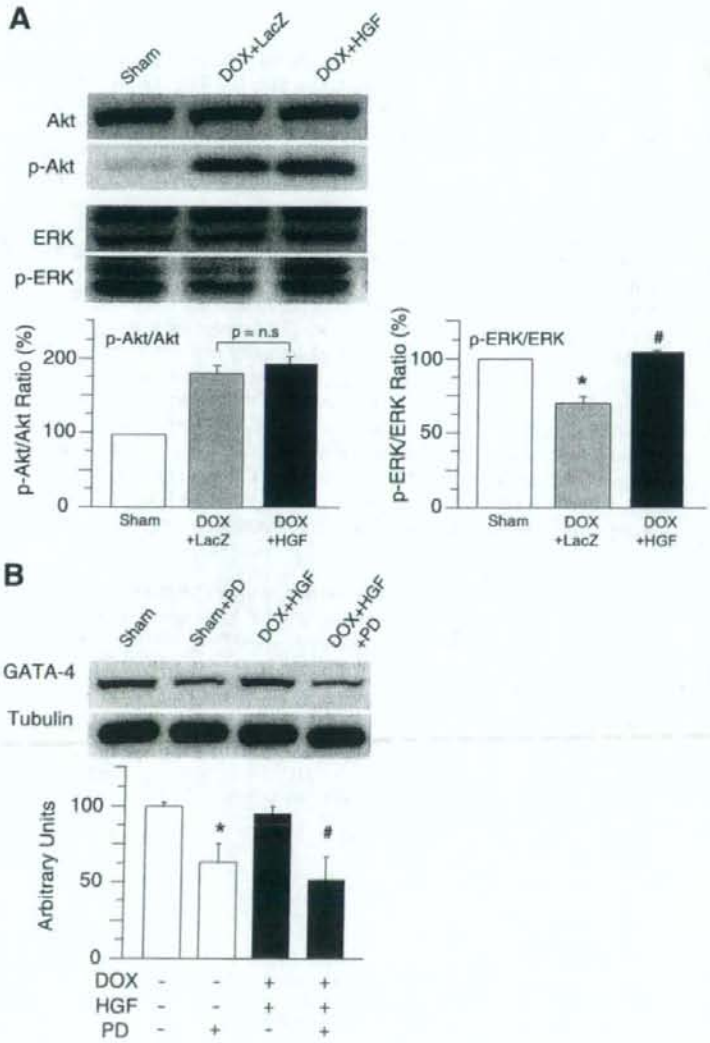

Fig. 7. *A*: Western blot analysis of the effects of hHGF gene transfer on myocardial expression of phosphorylated (p)-Akt and p-ERK. Activity of Akt and ERK is expressed, respectively, as the p-Akt-to-total Akt and p-ERK-to-total ERK ratio. *$P < 0.05$ vs. sham group; #$P < 0.05$ vs. the Dox + LacZ group. *B*: effect of the p42/p44 MAPK inhibitor PD-98059 (PD) on Dox-induced cardiomyopathy (*protocol 2*). Western blot and densitometric analyses of the effect of PD on myocardial expression of GATA-4. *$P < 0.05$ vs. control group; #$P < 0.05$ vs. Dox + HGF group.

and that effect was significantly attenuated by hHGF treatment (Fig. 7*A*).

To further examine the role played by ERK activation in mediating the cardioprotective effects of hHGF, we next tested the effect of inhibiting ERK activation using the MEK1-p42/p44 MAPK-specific inhibitor PD-98059 (*protocol 2*). When administered to mice along the hHGF gene, PD-98059 suppressed the hHGF-mediated reversal of doxorubicin's inhibition of GATA-4 expression (Fig. 7*B*). Moreover, PD-98059 significantly suppressed the HGF-mediated improvement in cardiac function and histology, i.e., the increase in cardiomyocyte size and the reduction in myocardial fibrosis (Table 1). This suggests that the ERK pathway is critically involved in the protective effect exerted by hHGF against doxorubicin-induced cardiomyopathy.

DISCUSSION

The present study provides clear evidence of the beneficial effects of HGF gene delivery on the cardiac dysfunction associated with doxorubicin-induced cardiomyopathy, a nonischemic cardiomyopathy. The principal pathological findings were that HGF prevented doxorubicin-induced atrophic degeneration of cardiomyocytes and myocardial fibrosis. The mechanism of action of HGF in this model differs from that seen in cases of myocardial infarction, where HGF reportedly enhances the survival of ischemic cardiomyocytes (27, 36). Notably, HGF exerted its therapeutic effects despite the fact that the cardiomyopathy was well established.

Mechanisms underlying the cardioprotective effects of HGF. Our findings suggest that several factors contribute to the cardioprotective effects of HGF against doxorubicin-induced cardiomyopathy. The first is that HGF mitigates the evoked atrophic degeneration of cardiomyocytes. The sarcomeric protein MHC is important for the structural integrity and function of cardiomyocytes, and its myocardial expression is reportedly downregulated by doxorubicin (11), an effect we confirmed in the present study. Our new finding is that HGF significantly restored the expression of both MHC and GATA-4 in the presence of doxorubicin. We suggest that GATA-4 is crucially involved in the antiatrophic effect of HGF, since GATA-4 is known to be a key regulator of heart development, to regulate myocardial expression of MHC and troponin I (22, 23) and to be depleted in doxorubicin-induced cardiotoxicity (4). Our results not only confirm those earlier findings but also demonstrate that HGF restores GATA-4 expression, even in the presence of doxorubicin.

c-Met/HGF receptor signaling is known to activate ERK/MAPK and PI3K/Akt signaling pathways (9, 24), both of which are implicated in myocardial hypertrophy (2, 5). Our findings suggest that altered signaling via ERK, but not Akt, is involved in doxorubicin-induced cardiomyopathy, which is consistent with a recent study showing that ERK activation is significantly diminished during the chronic stage of doxorubicin-induced cardiomyopathy (3 wk after doxorubicin administration) (20). Given that another study, in which isolated rat heart was subjected to excessive LV wall stress (induced by balloon inflation), showed MAPK (p38 and ERKs) to be involved in the activation of GATA-4 binding to DNA (35), we suggest that HGF exerts its cardioprotective effects by restoring activity in ERK/MAPK signaling pathway.

The HGF gene therapy significantly restored the doxorubicin-induced decrease in c-Met/HGF receptor expression in the heart, which is compatible with previous findings (18, 27): the increase in c-Met may be related to the autoinduction of gene expression triggered by HGF (27). However, immunohistochemistry showed cytoplasmic staining although c-Met is a membrane protein. One possible explanation for this discrepancy is the thickness of the sections (4 μm) relative to myocyte size (12 μm). A second possible explanation is the diffusion of diaminobenzidine products during the staining procedure. It is also possible that cytoplasmic staining is not an artifact but rather represents an abnormal distribution of excessive protein. Thus further studies are desirable in the future on the subcellular localization of c-Met in cardiomyocytes at the electron microscopic level.

Recent findings suggest that apoptosis among cardiomyocytes is a leading cause of cardiac dysfunction in doxorubicin-induced cardiomyopathy (13, 36). This hypothesis remains controversial, however, because the cardiomyocytes in question do not show the typical apoptotic morphology (16, 17, 30, 38). Seeking evidence of doxorubicin-induced apoptosis/cell death, we previously conducted a series of TUNEL assays,

Table 1. *Effects of inhibiting ERK activity with PD-98059 on LV function and histology 4 wk after administering saline or doxorubicin followed by LacZ or human HGF gene therapy: protocol 2*

	Sham (*protocol 1*)	Sham + PD-98059	Dox + HGF (*protocol 1*)	Dox + HGF + PD-98059
n	11	7	9	7
Function				
LVDd, mm	3.78±0.12	3.79±0.03	3.77±0.10	3.93±0.09
LVFS, %	29.2±1.61	30.7±0.42	25.2±1.08	20.9±0.96*
+dP/d*t*, mmHg/s	7,708±845	6,596±1,075	8,27±936	5,012±607*
−dP/d*t*, mmHg/s	−6,568±364	−6,355±976	−8,524±718	−5,434±779*
LVSP, mmHg	80.5±2.21	73.5±5.40	93.9±4.36	70.4±5.85*
Heart rate, beats/min	512±37	523±60	520±36	492±24
Histology				
Myocyte size, μm	13.8±0.37	13.5±0.20	13.4±0.18	12.4±0.32*
Fibrosis, %	0.55±0.04	0.48±0.04	0.58±0.04	0.69±0.01*
Flk-1$^+$ vessels/HPF	279±37.9	272±23.2	306±60.4	272±31.8
CD45$^+$ cells/HPF	0±0	0±0	0.02±0.04	0±0

Values are means ± SE; *n*, number of animals/group. Dox, doxorubicin; HGF, hepatocyte growth factor; LVDd, left ventricular (LV) end-diastolic diameter; LVFS, LV fractional shortening; ±dP/d*t*, maximum and minimum first derivative of pressure; LVSP, LV peak systolic pressure; HPF, high-power field. *$P <$ 0.05 vs. corresponding group without PD-98059 treatment.

electron microscopic examinations, and analyses of myocardial caspase-3 activation in the same animal model, but we detected no effect of doxorubicin on the incidence of apoptosis/cell death (17). We have now confirmed those findings. In the present study, mice received a single dose of doxorubicin, and the survival rate was 100% in all groups. This suggests the doxorubicin insult may have been too weak to induce cardiac cell death and weaker than the insults induced in earlier models. This may also hold true for our in vitro model.

HGF has been reported to be angiogenic (18, 28, 34), but we detected no doxorubicin-induced reduction in capillary density, nor did HGF promote capillary outgrowth, indicating that angiogenesis likely plays no mechanistic role in doxorubicin-induced cardiomyopathy or the cardioprotective effects of HGF.

Limitations of the study. We observed that doxorubicin stimulates the development of myocardial fibrosis and that HGF suppresses this pathological process. Although TGF-β1 is a potent stimulator of fibrosis in the failing heart, its involvement in doxorubicin-induced cardiomyopathy was challenged in a recent report (19). Consistent with that report, we found no significant doxorubicin-induced changes in the expression of TGF-β1. Therefore, although several studies suggest the mechanism underlying the antifibrotic effect of HGF is related, at least in part, to the inhibition of TGF-β1 secretion (28, 34), in the case of doxorubicin-induced cardiomyopathy, HGF appears to diminish fibrosis via a different mechanism. It is also known that doxorubicin induces cardiac expression of cyclooxygenase-2 (1), which occupies a central position in the biosynthesis of proinflammatory prostaglandin E_2, prostacyclin and thromboxane A_2, and that inhibition of cyclooxygenase-2 improves cardiac function in a model of doxorubicin-induced cardiomyopathy (10). Actually, we previously observed expression of cyclooxygenase-2 to be upregulated 2 wk after doxorubicin injection, but that is a more acute stage than the one studied here (16, 17). We did not see greater expression of cyclooxygenase-2 in the present 4-wk model, where significant infiltration of inflammatory cells also was not seen. Still, we cannot exclude the possibility that cyclooxygenase-2 contributes to the etiology of myocardial fibrosis in doxorubicin-induced cardiomyopathy. Our results also indicate that ERK inhibition blocks the antifibrotic effect of HGF in the present model; thus, further investigation will be needed to precisely define the mechanisms operating.

HGF reportedly exerts myocardial regeneration by mobilizing bone marrow-derived cells to the myocardium (15), and cardiac stem cells reportedly express c-Met/HGF receptors (12, 37). Although we did not directly evaluate the contribution made by cardiomyocyte regeneration (either from bone marrow cells or cardiac stem cells) to the beneficial effects of HGF, our immunohistochemical analysis of Ki-67, which showed an absence of cardiomyocyte proliferation, suggests that it is unlikely that cardiomyocyte regeneration plays a role in the present model. This result of ours seems to be in contrast with the previous study by Iwasaki et al. (12), which reported enhanced cardiomyocyte proliferation and increased Sca1-positive cardiac progenitor cells in doxorubicin-induced cardiomyopathy by a specific delivering method of HGF (intravenous injection of HGF delivered by ultrasound-mediated destruction of microbubbles). In addition, the peak plasma HGF concentration should have been widely different between the studies. Iwasaki et al. (12) intravenously gave 10 μg of HGF per animal (~20 g body wt), whereas in our study the plasma HGF concentration attained 3 days after gene delivery was 3.25 ± 0.85 ng/ml. These methodological differences might have a strong bearing on the different observations between the studies. Further studies are needed to focus specifically on the biological effect of HGF on stem cells.

Conclusion. The present study provides the first evidence of the beneficial effects of HGF gene transfer in doxorubicin-induced cardiomyopathy. These effects include the attenuation of atrophic degeneration of cardiomyocytes and the reduction of myocardial fibrosis, accompanied by the restoration of myocardial expression of GATA-4 and sarcomeric proteins. Our findings also suggest that HGF-mediated ERK activation is associated with these beneficial effects and may thus underlie the cardioprotection provided by HGF gene transfer.

ACKNOWLEDGMENTS

We thank Hatsue Ohshika, Akiko Tsujimoto, and the staff of the Department of Food Science, Kyoto Women's University, for technical assistance.

REFERENCES

1. **Adderley SR, Fitzgerald DJ.** Oxidative damage of cardiomyocytes is limited by extracellular regulated kinases 1/2-mediated induction of cyclooxygenase-2. *J Biol Chem* 274: 5038–5046, 1999.
2. **Akiyama Y, Ashizawa N, Seto S, Ohtsuru A, Kuroda H, Ito M, Yamashita S, Yano K.** Involvement of receptor-type tyrosine kinase gene families in cardiac hypertrophy. *J Hypertens* 17: 1329–1337, 1999.
3. **Aoyama T, Takemura G, Maruyama R, Kosai K, Takahashi T, Koda M, Hayakawa K, Kawase Y, Minatoguchi S, Fujiwara H.** Molecular mechanisms of non-apoptosis by Fas stimulation alone versus apoptosis with an additional actinomycin D in cultured cardiomyocytes. *Cardiovasc Res* 55: 787–798, 2002.
4. **Aries A, Paradis P, Lefebvre C, Schwartz RJ, Nemer M.** Essential role of GATA-4 in cell survival and drug-induced cardiotoxicity. *Proc Natl Acad Sci USA* 101: 6975–6980, 2004.
5. **Birchmeier C, Gherardi E.** Developmental roles of HGF/SF and its receptor, the c-Met tyrosine kinase. *Trends Cell Biol* 8: 404–410, 1998.
6. **Bottaro DP, Rubin JS, Faletto DL, Chan AM, Kmiecik TE, Vande Woude GF, Aaronson SA.** Identification of the hepatocyte growth factor receptor as the c-met proto-oncogene product. *Science* 251: 802–804, 1991.
7. **Chen SH, Chen XH, Wang Y, Kosai K, Finegold MJ, Rich SS, Woo SL.** Combination gene therapy for liver metastasis of colon carcinoma in vivo. *Proc Natl Acad Sci USA* 92: 2577–2581, 1995.
8. **Cuenda A, Alessi DR.** Use of kinase inhibitors to dissect signaling pathways. *Methods Mol Biol* 99: 161–175, 2000.
9. **Day RM, Cioce V, Breckenridge D, Castagnino P, Bottaro DP.** Differential signaling by alternative HGF isoforms through c-Met: activation of both MAP kinase and PI 3-kinase pathways is insufficient for mitogenesis. *Oncogene* 18: 3399–3406, 1999.
10. **Delgado RM 3rd, Nawar MA, Zewail AM, Kar B, Vaughn WK, Wu KK, Aleksic N, Sivasubramanian N, McKay K, Mann DL, Willerson JT.** Cyclooxygenase-2 inhibitor treatment improves left ventricular function and mortality in a murine model of doxorubicin-induced heart failure. *Circulation* 109: 1428–1433, 2004.
11. **Ito H, Miller SC, Billingham ME, Akimoto H, Torti SV, Wade R, Gahlmann R, Lyons G, Kedes L, Torti FM.** Doxorubicin selectively inhibits muscle gene expression in cardiac muscle cells in vivo *and* in vitro. *Proc Natl Acad Sci USA* 87: 4275–4279, 1990.
12. **Iwasaki M, Adachi Y, Nishiue T, Minamino K, Suzuki Y, Zhang Y, Nakano K, Koike Y, Wang J, Mukaide H, Taketani S, Yuasa F, Tsubouchi H, Gohda E, Iwasaka T, Ikehara S.** Hepatocyte growth factor delivered by ultrasound-mediated destruction of microbubbles induces proliferation of cardiomyocytes and amelioration of left ventricular contractile function in doxorubicin-induced cardiomyopathy. *Stem Cells* 23: 1589–1597, 2005.
13. **Kitta K, Day RM, Ikeda T, Suzuki YJ.** Hepatocyte growth factor protects cardiac myocytes against oxidative stress-induced apoptosis. *Free Radic Biol Med* 31: 902–910, 2001.

14. **Kosai K, Matsumoto K, Funakoshi H, Nakamura T.** Hepatocyte growth factor prevents endotoxin-induced lethal hepatic failure in mice. *Hepatology* 30: 151–159, 1999.
15. **Kucia M, Dawn B, Hunt G, Guo Y, Wysoczynski M, Majka M, Ratajczak J, Rezzoug F, Ildstad ST, Bolli R, Ratajczak MZ.** Cells expressing early cardiac markers reside in the bone marrow and are mobilized into the peripheral blood after myocardial infarction. *Circ Res* 95: 1191–1199, 2004.
16. **Li L, Takemura G, Li Y, Miyata S, Esaki M, Okada H, Kanamori H, Khai NC, Maruyama R, Ogino A, Minatoguchi S, Fujiwara T, Fujiwara H.** Preventive effect of erythropoietin on cardiac dysfunction in doxorubicin-induced cardiomyopathy. *Circulation* 113: 535–543, 2006.
17. **Li L, Takemura G, Li Y, Miyata S, Esaki M, Okada H, Kanamori H, Ogino A, Maruyama R, Nakagawa M, Minatoguchi S, Fujiwara T, Fujiwara H.** Granulocyte colony-stimulating factor improves left ventricular function of doxorubicin-induced cardiomyopathy. *Lab Invest* 87: 440–455, 2007.
18. **Li Y, Takemura G, Kosai K, Yuge K, Nagano S, Esaki M, Goto K, Takahashi T, Hayakawa K, Koda M, Kawase Y, Maruyama R, Okada H, Minatoguchi S, Mizuguchi H, Fujiwara T, Fujiwara H.** Postinfarction treatment with an adenoviral vector expressing hepatocyte growth factor relieves chronic left ventricular remodeling and dysfunction in mice. *Circulation* 107: 2499–2506, 2003.
19. **Lou H, Danelisen I, Singal PK.** Cytokines are not upregulated in adriamycin-induced cardiomyopathy and heart failure. *J Mol Cell Cardiol* 36: 683–690, 2004.
20. **Lou H, Danelisen I, Singal PK.** Involvement of mitogen-activated protein kinases in adriamycin-induced cardiomyopathy. *Am J Physiol Heart Circ Physiol* 288: H1925–H1930, 2005.
21. **Mizuguchi H, Kay AM.** A simple method for constructing E1- and E1/E4-deleted recombinant adenoviral vectors. *Hum Gene Ther* 10: 2013–2017, 1999.
22. **Molkentin JD, Kalvakolanu DV, Markham BE.** Transcription factor GATA-4 regulates cardiac muscle-specific expression of the alpha-myosin heavy-chain gene. *Mol Cell Biol* 14: 4947–4957, 1994.
23. **Murphy AM, Thompson WR, Peng LF, Jones L 2nd.** Regulation of the rat cardiac troponin I gene by the transcription factor GATA-4. *Biochem J* 322: 393–401, 1997.
24. **Nakagami H, Morishita R, Yamamoto K, Taniyama Y, Aoki M, Matsumoto K, Nakamura T, Kaneda Y, Horiuchi M, Ogihara T.** Mitogenic and antiapoptotic actions of hepatocyte growth factor through ERK, STAT3, and AKT in endothelial cells. *Hypertension* 37: 581–586, 2001.
25. **Nakamura T, Nawa K, Ichihara A.** Partial purification and characterization of hepatocyte growth factor from serum of hepatectomized rats. *Biochem Biophys Res Commun* 122: 1450–1459, 1984.
26. **Nakamura T, Nishizawa T, Hagiya M, Seki T, Shimonishi M, Sugimura A, Tashiro K, Shimizu S.** Molecular cloning and expression of human hepatocyte growth factor. *Nature* 342: 440–443, 1989.
27. **Nakamura T, Mizuno S, Matsumoto K, Sawa Y, Matsuda H, Nakamura T.** Myocardial protection from ischemia/reperfusion injury by endogenous and exogenous HGF. *J Clin Invest* 106: 1511–1519, 2000.
28. **Nakamura T, Matsumoto K, Mizuno S, Sawa Y, Matsuda H, Nakamura T.** Hepatocyte growth factor prevents tissue fibrosis, remodeling, and dysfunction in cardiomyopathic hamster hearts. *Am J Physiol Heart Circ Physiol* 288: H2131–H2139, 2005.
29. **Olson RD, Mushlin P.** Doxorubicin cardiotoxicity: analysis of prevailing hypotheses. *FASEB J* 4: 3076–3086, 1990.
30. **Rosenoff SH, Olson HM, Young DM, Bostick F, Young RC.** Adriamycin-induced cardiac damage in the mouse: a small-animal model of cardiotoxicity. *J Natl Cancer Inst* 55: 191–194, 1975.
31. **Simpson C, Herr H, Courville KA.** Concurrent therapies that protect against doxorubicin-induced cardiomyopathy. *Clin J Oncol Nurs* 8: 497–501, 2004.
32. **Singal PK, Iliskovic N.** Doxorubicin-induced cardiomyopathy. *N Engl J Med* 339: 900–905, 1998.
33. **Sparano JA.** Use of dexrazoxane and other strategies to prevent cardiomyopathy associated with doxorubicin-taxane combinations. *Semin Oncol* 125, *Suppl* 10: 66–71, 1998.
34. **Taniyama Y, Morishita R, Aoki M, Hiraoka K, Yamasaki K, Hashiya N, Matsumoto K, Nakamura T, Kaneda Y, Ogihara T.** Angiogenesis and antifibrotic action by hepatocyte growth factor in cardiomyopathy. *Hypertension* 40: 47–53, 2002.
35. **Tenhunen O, Sarman B, Kerkela R, Szokodi I, Papp L, Toth M, Ruskoaho H.** Mitogen-activated protein kinases p38 and ERK 1/2 mediate the wall stress-induced activation of GATA-4 binding in adult heart. *J Biol Chem* 279: 24852–24860, 2004.
36. **Ueda H, Nakamura T, Matsumoto K, Sawa Y, Matsuda H, Nakamura T.** A potential cardioprotective role of hepatocyte growth factor in myocardial infarction in rats. *Cardiovasc Res* 51: 41–50, 2001.
37. **Urbanek K, Rota M, Cascapera S, Bearzi C, Nascimbene A, De Angelis A, Hosoda T, Chimenti S, Baker M, Limana F, Nurzynska D, Torella D, Rotatori F, Rastaldo R, Musso E, Quaini F, Leri A, Kajstura J, Anversa P.** Cardiac stem cells possess growth factor-receptor systems that after activation regenerate the infarcted myocardium, improving ventricular function and long-term survival. *Circ Res* 97: 663–673, 2005.
38. **Zhang J, Clark JR Jr, Herman EH, Ferrans VJ.** Doxorubicin-induced apoptosis in spontaneously hypertensive rats: differential effects in heart, kidney and intestine, and inhibition by ICRF-187. *J Mol Cell Cardiol* 28: 1931–1943, 1996.

最新学際情報

増殖制御型アデノウイルスによる遺伝子治療

癌はいまだわが国を含む多くの先進諸国の最多死因であり，わが国だけでも毎年約32万人が癌で死亡している。つまり近年に治療成績の向上がみられる早期癌とは対照的に，多発性遠隔転移の進行癌にはいまだ効果的な治療法は確立されておらず，そのため遺伝子治療のような革新的治療法の開発が切望されている。

遺伝子治療の臨床成績は，まず90年代にレトロウイルスベクターによる*ex vivo*遺伝子治療（切除癌に*in vitro*の培養下でサイトカインなどの治療遺伝子を導入し，放射線で増殖不能化したのちに体内に戻す）が行われた。しかしこれは不十分な治療効果に加え，多大な労力に伴う治療の不確実性と高額の経費の問題もあり，一般医薬化には至っていない。

90年代後半より，*in vivo*遺伝子導入（直接癌部にベクター注入）を可能とする非増殖型アデノウイルス（ADV）ベクターが，癌遺伝子治療の中心ベクターとなり，臨床試験数も増加してきた[1]。現在まで世界で約1,300の遺伝子治療の臨床プロトコールが発表されているが，その2/3は癌であり，使用されているベクターはADVが最多である。このような臨床試験（研究）での結論は，「遺伝子治療は癌には安全な一般医薬となりうるが，治療効果は当初期待されたレベルには達していない」ということである。この原因の1つは，「非」増殖型のベクターでは*in vivo*で体内の全癌細胞にもれなく治療遺伝子を導入することは「物理的に」不可能であるため，癌の再発が起こりえるという問題である。

この問題を克服するため，現在世界中で盛んに研究が進められているのが，癌特異的増殖型ADV（CRA）である。CRAは，ウイルス増殖が正常細胞では阻止され，癌細胞内では旺盛に起こるように遺伝子改変されたADVで，生体内で効率的かつ癌細胞特異的な遺伝子導入が可能となる[2]。またさらにCRA自身が，増幅したウイルス（蛋白）により癌細胞を特異的に殺す「溶解性ウイルス」医薬となる利点も併せもつ。その原理は，非増殖型ADVではウイルス増殖に必須のE1領域を欠損させて治療遺伝子に置換していたが，CRAではE1領域を改変（一部欠失変異化と，内因性プロモーターの置換の2戦略あり）することで，ウイルス増殖が癌のみで起こるようにするというものである[2]。CRAは基礎研究，臨床研究の両方でその有用性が示されている一方で，完全に理想的なCRAを開発するためには，2つの問題が残っていた。第1には，このような一因子で癌と正常の細胞を完全に識別するレベルの癌特異化は困難ということである。また最大の問題は，このような一因子制御のCRAでさえ，効率的・標準化作製技術が確立されていないため，研究開発がきわめて非効率ということであった。

著者らはこの問題を克服するため，従来の単一因子のCRAとは一線を画く「多数」の異なる癌特異化因子で，精密なウイルス増殖制御が可能なCRAであるm-CRAを，迅速・効率的に作製可能な「標準化」作製技術を初めて開発した[3]。その原理と作製法の詳細は拙著[2,3]に譲るが，これにより7因子以上の癌特異化因子を挿入する次世代のm-CRAが作製可能となった。

著者らはこの独自技術でさまざまな癌治療m-CRA医薬を作製，評価しているが，本稿ではサバイビン依存性m-CRAを紹介する[4]。サバイビンはIAP（inhibitor of apoptosis）ファミリーとして同定されたが，その後，骨軟部腫瘍を含むほとんどの種類の癌で高発現している一方，分化した正常細胞では発現が認められないことがわかり，現在は癌治療のターゲット分子としても注目されている。著者らはこのサバイビン遺伝子プロモーターでADVのE1を発現制御する

0286-5394/08/¥400/論文/JCLS

Surv.m-CRAを開発した。

Surv.m-CRAは調べた全種類の癌細胞で，癌細胞特異的なウイルス増殖と細胞死を誘導し，さらに骨肉腫の動物モデルで高い治療効果を示した。さらに既報告のCRAのなかでは最良のテロメラーゼ(TERT)依存性m-CRA(Tert.m-CRA)と詳細な比較実験をしたところ，Surv.m-CRAはTert.m-CRAを，癌治療効果と癌特異性(安全性)の両面でしのぐという有望な成果が得られた[2),4)]。このように骨軟部腫瘍はもとより，ほぼ全種類の癌を効率よく安全に治療でき，既存のm-CRAより優れたSurv.m-CRAは，早期の臨床応用化が期待される。また，癌特異性(安全性)も癌治療効果もさらに増殖した高度m-CRA化の種々の改良型Surv.m-CRA，あるいは第二，第三弾の新規m-CRAの開発も進めている。

将来のわが国の国民福祉と経済の向上につながるのは，「基盤技術からわが国で開発し，基本特許の知財を確保した医薬」であるため，著者らのm-CRAの医薬化は重要であると思われる。遺伝子治療の臨床化の公的支援の体制が十分でないわが国では困難もあるが，著者ら自身でのm-CRA医薬開発と併せて，わが国全体のm-CRA研究開発の発展に寄与できる体制づくりや産業化も計画している。(堀川良治／小宮節郎 鹿児島大学大学院医歯学総合研究科運動機能修復学講座整形外科学，小戝健一郎　鹿児島大学大学院医歯学総合研究科細胞生物構造学講座)

文　献

1)Chen SH, Chen XH, Wang Y, Kosai K, et al：Combination gene therapy for liver metastasis of colon carcinoma *in vivo*. Proc Natl Acad Sci USA,1995; 92：2577-2581, 1995.

2)室伏善照，神圃純一，小戝健一郎：新世代癌遺伝子治療のための多因子で増殖制御/癌特異化するアデノウイルスの作製法．細胞工学，25：60-66，2005.

3)Nagano S, Oshika H, Fujiwara H, Komiya S, Kosai K, et al：An efficient construction of conditionally replicating adenoviruses that target tumor cells with multiple factors. Gene Ther, 2005.

4)Kamizono J, Nagano S, Murofushi Y, Komiya S, Kosai K, et al：Survivin-responsive conditionally replicating adenovirus exhibits cancer-specific and efficient viral replication. Cancer Res, 65：5284-5291, 2005.

Available online at www.sciencedirect.com
ScienceDirect
Bioorganic & Medicinal Chemistry Letters 18 (2008) 2499–2504
Bioorganic & Medicinal Chemistry Letters

Sugar Chips immobilized with synthetic sulfated disaccharides of heparin/heparan sulfate partial structure☆

Masahiro Wakao,[a] Akihiro Saito,[a] Koh Ohishi,[a] Yuko Kishimoto,[b] Tomoaki Nishimura,[a,b] Michael Sobel[c] and Yasuo Suda[a,b,*]

[a]*Department of Nanostructure and Advanced Materials, Graduate School of Science and Engineering, Kagoshima University, 1-21-40 Korimoto, Kagoshima 890-0065, Japan*
[b]*SUDx-Biotec corporation, 5-5-2 Minatojima-cho, Kobe 650-0047, Japan*
[c]*Department of Surgery, University of Washington and VA Puget Sound Health Care System, Seattle, WA 98108, USA*

Received 21 August 2007; revised 24 December 2007; accepted 16 January 2008
Available online 19 January 2008

Abstract—Carbohydrate chip technology has a great potential for the high-throughput evaluation of carbohydrate–protein interactions. Herein, we report syntheses of novel sulfated oligosaccharides possessing heparin and heparan sulfate partial disaccharide structures, their immobilization on gold-coated chips to prepare array-type Sugar Chips, and evaluation of binding potencies of proteins by surface plasmon resonance (SPR) imaging technology. Sulfated oligosaccharides were efficiently synthesized from glucosamine and uronic acid moieties. Synthesized sulfated oligosaccharides were then easily immobilized on gold-coated chips using previously reported methods. The effectiveness of this analytical method was confirmed in binding experiments between the chips and heparin binding proteins, fibronectin and recombinant human von Willebrand factor A1 domain (rh-vWf-A1), where specific partial structures of heparin or heparan sulfate responsible for binding were identified.
© 2008 Elsevier Ltd. All rights reserved.

Carbohydrate chips and related array technologies[1–3] have attracted a great deal of attention as a powerful tool for glycomics. Like DNA[4] and protein chips,[5] they can rapidly and simply evaluate carbohydrate–protein interactions in parallel, with a minimum amount of sample. Our ongoing research involves this functional analysis of sulfated polysaccharides such as heparin (HP) and heparan sulfate (HS).[3a] HP and HS are highly sulfated polysaccharides and belong to the glycosaminoglycan (GAG) superfamily. They are among the most complex of carbohydrates, and play a significant role in biological processes through their binding interactions with numerous proteins,[6] such as growth factors, cytokines, viral proteins, and coagulation factors, among others. HP/HS have a basic structure composed of a repeating α or β(1,4)-linked disaccharide moiety which is derived from uronic acid (either glucuronic acid or iduronic acid) and *N*-acetyl-glucosamine residues. In general, HP/HS chains are very heterogeneous and contain innumerable substitution patterns due in part to some randomness in the multiple enzymatic modifications in their biosynthesis. This heterogeneity makes it difficult to elucidate the structure-function relationships of HP/HS at the molecular level. Therefore, structurally defined HP/HS sequences are necessary for the precise elucidation of the mode of HP/HS actions on their target molecules. So far, many synthetic efforts have been dedicated to the synthesis of HP/HS fragments.[3b–d,7,8]

Previously, we have reported that a specific disaccharide unit in HP, *O*-(2-deoxy-2-sulfamido-6-*O*-sulfo-α-D-glucopyranosyl)-(1-4)-2-*O*-sulfo-α-L-idopyranosyluronic acid (abbreviated as GlcNS6S-IdoA2S), is a key unit for binding to human platelets[9] and von Willebrand factor (vWf),[10] and that the clustering of these disaccharides significantly enhanced the interaction.[11,12] To systematically investigate heparin's binding properties, we have developed a method[3a] for the immobilization the sulfated oligosaccharide onto a gold-coated chip,

Keywords: Sugar; Carbohydrate; Chip; Heparin; Heparan sulfate; Carbohydrate–protein interaction; Surface plasmon resonance; SPR; SPR-imaging.

☆ Syntheses of sulfated oligosaccharide of heparin and heparan sulfate partial structures and their application to Sugar Chips are described.

* Corresponding author. Tel./fax: +81 99 285 8369; e-mail: ysuda@eng.kagoshima-u.ac.jp

0960-894X/$ - see front matter © 2008 Elsevier Ltd. All rights reserved.
doi:10.1016/j.bmcl.2008.01.069

and have devised an analytical system using surface plasmon resonance (SPR) technology, which permits their real-time study without further labeling. These systems can be applied to the investigation of the binding interactions of a variety of structurally defined oligosaccharides.

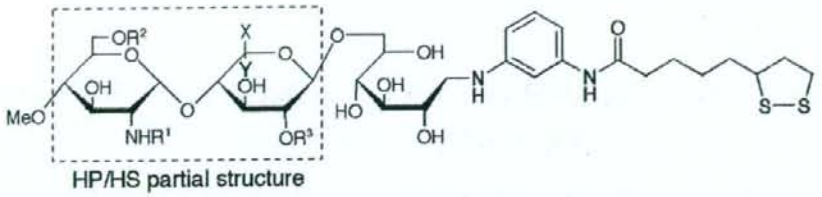

1, GlcNS6S-IdoA2S: $R^1=SO_3^-$, $R^2=SO_3^-$, $R^3=SO_3^-$, X=H, $Y=CO_2^-$
2, GlcNS-IdoA2S: $R^1=SO_3^-$, R^2=H, $R^3=SO_3^-$, X=H, $Y=CO_2^-$
3, GlcNS6S-GlcA: $R^1=SO_3^-$, $R^2=SO_3^-$, R^3=H, $X=CO_2^-$, Y=H
4, GlcNS-GlcA: $R^1=SO_3^-$, R^2=H, R^3=H, $X=CO_2^-$, Y=H

Figure 1. Sulfated disaccharide partial structures of heparin/heparan sulfate.

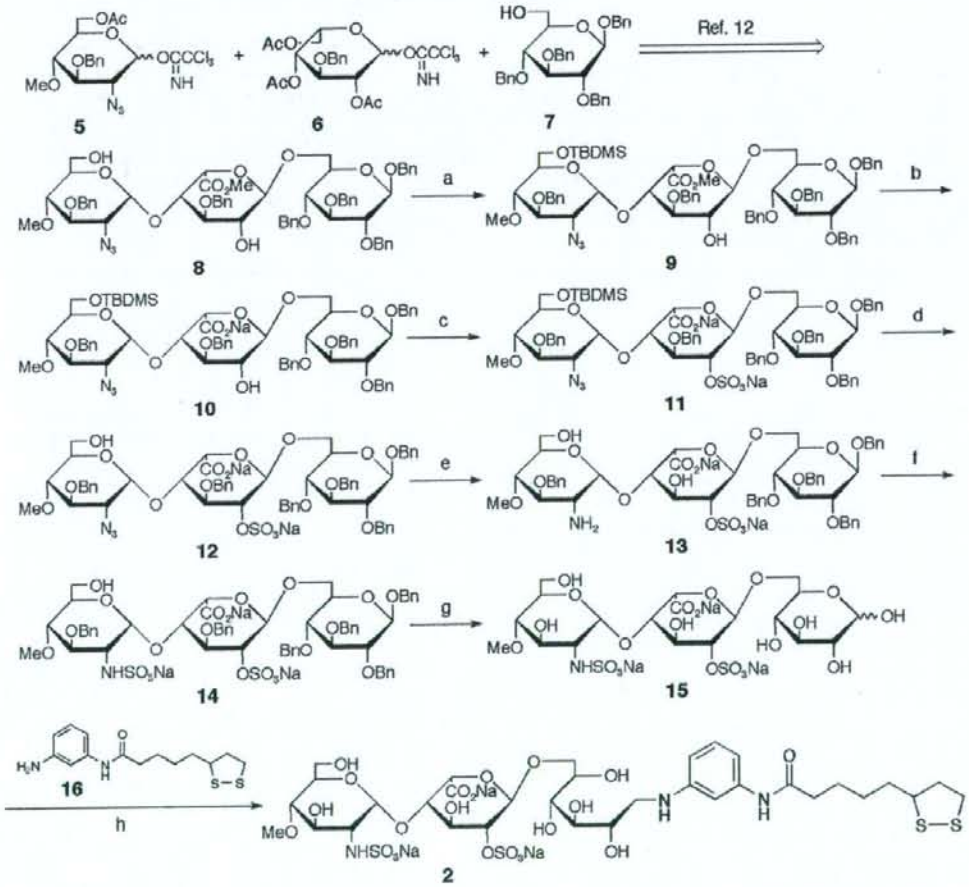

Scheme 1. Synthesis of ligand conjugate **2** containing GlcNS-IdoA2S. Reagents: (a) TBDMSCl, imidazole, MS4AP in CH_2Cl_2, 45%; (b) 1 M NaOH, MeOH/THF (1:1), 70%; (c) SO_3Pyr in Pyr; (d) HFPyr in Pyr; (e) 10% Pd–C, H_2 (1 kg/cm^2) in THF/MeOH (2:1); (f) SO_3Pyr in H_2O; (g) 10% Pd–C, H_2 (7 kg/cm^2) in H_2O/AcOH (5:1), 29% (5 steps); (h) $NaBH_3CN$ in DMAc/H_2O/AcOH (1:1:0.1), 82%.

To better understand the HP/HS disaccharide structures involved in specific protein interactions, we designed three kinds of sulfated trisaccharide ligand conjugates **2**–**4** containing the disaccharide units as shown in Figure 1; GlcNS-IdoA2S (**2**): *O*-(2-deoxy-2-sulfamido-α-D-glucopyranosyl)-(1-4)-2-*O*-sulfo-α-L-idopyranosyluronic acid, GlcNS6S-GlcA (**3**): *O*-(2-deoxy-2-sulfamido-6-*O*-sulfo-α-D-glucopyranosyl)-(1-4)-α-D-glucopyranosyluronic acid, GlcNS-GlcA (**4**): *O*-(2-deoxy-2-sulfamido-α-D-glucopyranosyl)-(1-4)-α-D-glucopranosyluronic acid. The disaccharide units contained in ligand conjugates **1**–**4** of Figure 1 are frequently found in HP/HS disaccharide unit.

For efficient synthesis, four monomeric building blocks were prepared. 2-Azido glucose derivative **5**, idose derivative **6**, and 4,6-benzylidene glucose derivative **17** were used for glucosamine, iduronic acid, and glucuronic acid moieties, respectively. Selective sulfation onto glucosamine and iduronic acid or glucuronic acid moieties can be carried out by an appropriate functionalization. The 6-OH glucose derivative **7** was used as the reducing end for the conjugation to linker molecule **16** after deprotection on the glucose, which works not only as a reducing end donor for reductive amination but also as the hydrophilic moiety in the molecule to minimize any non-specific hydrophobic interactions between the linker and target proteins or cells.

The synthesis of ligand conjugate **2** containing GlcNS-IdoA2S unit was carried out as shown in Scheme 1. Trisaccharide **8**, which was prepared according to the method reported previously,[12] was selectively protected by *t*-butyldimethylsilyl (TBDMS) group. The methyl ester of trisaccharide **9** was hydrolyzed and the remaining 2′-hy-

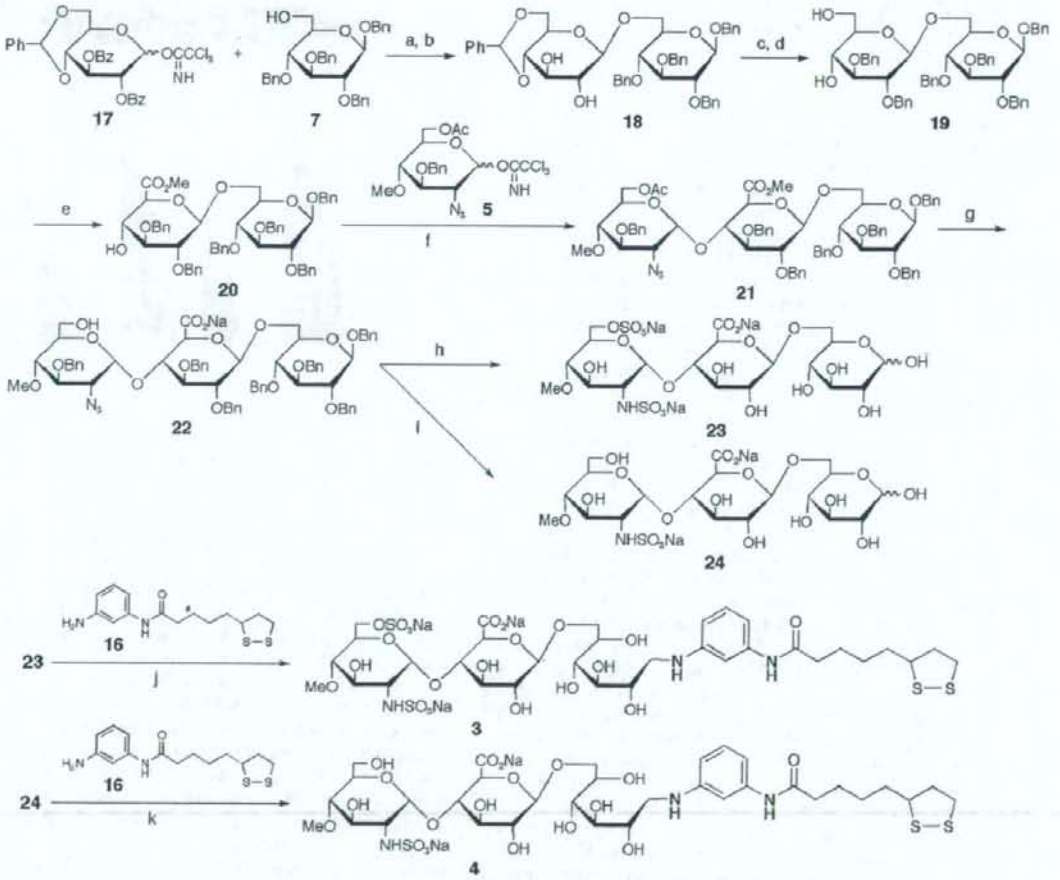

Scheme 2. Synthesis of ligand conjugates **3** and **4** containing GlcNS6S-GlcA and GlcNS-GlcA, respectively. Reagents and conditions: (a) BF_3OEt_2, MS4AP in CH_2Cl_2, −20 °C; (b) 0.1 M NaOMe, 90% (2 steps); (c) NaH, BnBr in DMF, 0 °C → rt, 88%; (d)16% TFA, 8% MeOH in CH_2Cl_2, 0 °C → rt, 93%; (e) TEMPO, KBr, NaClO in CH_2Cl_2; $TMSCHN_2$, 83% (2 steps); (f) TBDMSOTf, MS4AP in toluene, −20 °C, 84%; (g) 5 M NaOH in MeOH/THF (1:1), 89%; (h) SO_3Pyr in Pyr; 10% Pd–C, H_2 (1 kg/cm^2) in THF/H_2O (2:1); SO_3Pyr in H_2O (pH ≈ 9.5); 10% Pd–C, H_2 (7 kg/cm^2) in H_2O/AcOH (5:1), 28% (4 steps); (i) 10% Pd–C, H_2 (1 kg/cm^2) in THF/H_2O (2:1); SO_3Pyr in MeOH/H_2O (3:2); 10% Pd–C, H_2 (7 kg/cm^2) in H_2O/MeOH/AcOH (5:5:2), 39% (3 steps); (j) $NaBH_3CN$ in DMAc/H_2O/AcOH (1:1:0.1), 62%; (k) $NaBH_3CN$ in DMAc/H_2O/AcOH (1:1:0.1), 50%.

droxy group was sulfated using sulfur trioxide-pyridine complex at room temperature. After removing the TBDMS group with HFpyridine complex, the azido group was reduced using a catalytic amount of Pd-C under hydrogen atmosphere and the resulting amino group was *N*-sulfated. All benzyl protecting groups were removed by hydrogenolysis using catalytic Pd-C to give the desired trisaccharide **15**. Finally, the reductive amination of trisaccharide **15** with linker compound **16** was performed using $NaBH_3CN$ to afford the desired ligand conjugate **2** in good yield. Compound **2** was purified by gel-filtration chromatography with Sephadex G-25 fine and confirmed by ^1H NMR and ESI-TOF/MS analyses.[13]

The syntheses of ligand conjugates **3** and **4** were carried out in the same fashion as the syntheses of **1** and **2** (Scheme 2). Glycosylation of 6-OH glucose **7** and imidate **17** with trimethylsilyl trifluoromethanesulfonate (TMSOTf) as a promoter and treatment of the resultant with NaOMe gave disaccharide **18** in a good yield. The resulting hydroxy groups of **18** were then protected with a benzyl group. After removal of the benzylidene group, the primary 6′-OH group was selectively oxidized to carboxylic acid using 2,2,6,6-tetramethyl-1-piperidinyloxy (TEMPO).[14] The resulting carboxyl group was esterified with (trimethylsilyl)diazomethane to afford the disaccharide **20**. The 2-azido imidate **5** was condensed with disaccharide **20** using TBDMSOTf at −20 °C to give selectively an α-linked trisaccharide **21**.[11,15] Hydrolysis of the acetyl group and methyl ester was then carried out using aqueous NaOH to give the common intermediate **22** for trisaccharides **23** and **24**. The sulfated trisaccharide **23** was obtained by *O*-sulfation of the 6″-hydoxyl group and reduction and *N*-sulfation of 2′-azido group was followed by hydrogenolysis. Conversely, the sulfated trisaccharide **24** was prepared by the same method as the synthesis of trisaccharide **23**, omitting the *O*-sulfation. The ligand-conjugates **3**[16] and **4**[17] were synthesized in satisfactory yields as similar to the described procedure for compound **2**.

Binding interactions were investigated by use of the SPR imaging sensor.[18] When fibronectin was tested (Fig. 2), specific binding interactions were clearly observed with compounds **1** (GlcNS6S-IdoA2S, K_D = 5.5 nM) and **3** (GlcNS6S-GlcA, K_D = 6.5 nM), but not with compounds **2** (GlcNS-IdoA2S, K_D = 30 nM) and **4** (GlcNS-GlcA, K_D = 33 nM). These results indicate that the *N*-sulfation and 6-*O*-sulfation of glucosamine in HP/HS are important for fibronectin binding, while 2-*O*-sulfation of iduronic acid is less important. Recently, Couchman and coworkers showed that *N*-sulfation of glucosamine was essential for fibronectin binding and 2-*O*-sulfation of iduonic acid or 6-*O*-sulfation of glucosamine has marginal effects.[19] Additionally, *N*-sulfation and 6-*O*-sulfation of glucosamine were important for focal adhesion formation through syndecan-4, heparan sulfate proteoglycan. Our results are in agreement with those data.

In contrast, when recombinant human vWf A1 domain (rh-vWf-A1)[20] was injected over the chips, a different pattern of oligosaccharide binding preference was noted (Fig. 3). A strong interaction was observed with compounds **1** (GlcNS6S-IdoA2S, K_D = 1.0 μM) and **2** (GlcNS-IdoA2S, K_D = 0.9 μM). Weaker interaction was seen with compound **3** (GlcNS6S-GlcA, K_D = 1.4 μM), while distinctly low binding was observed with compound **4** (GlcNS-GlcA, K_D = 4.3 μM). Although the GlcNS6S-IdoA2S (**1**) disaccharide structure was considered a key binding domain of vWf,[10] the exact disaccharide structure responsible for vWf binding is still unclear. We found previously that clustered compounds containing three units of GlcNS6S-IdoA2S[12] possessed higher competitive binding activity compared to compounds containing less than two units of GlcNS6S-IdoA2S (unpublished data). Together with those data, the current results indicate that the tri-sulfated disaccharide binds vWf best, that loss of either the 6-sulfate of GlcN or the 2-sulfate of IdoA reduces vWf binding significantly, and that the *N*-sulfate of GlcN alone is not sufficient for binding vWf.

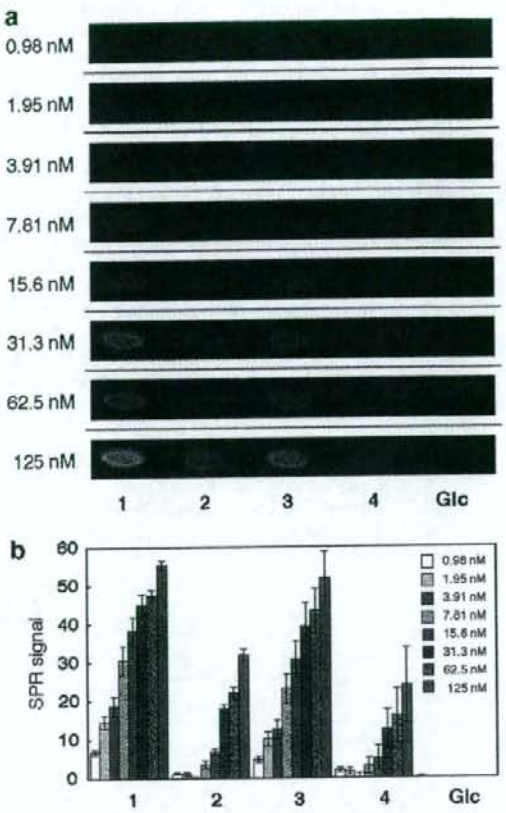

Figure 2. Binding study with fibronectin. (a) SPR difference imaging on the chip immobilized with compounds **1**, **2**, **3**, **4**, and Glcα(1-6)Glc-mono (Glc). Measurements were carried out with analyte in the range between 0.98 and 125 nM. (b) Bar graph profiles of different concentrations of protein. The error bars represent +/− SEM.

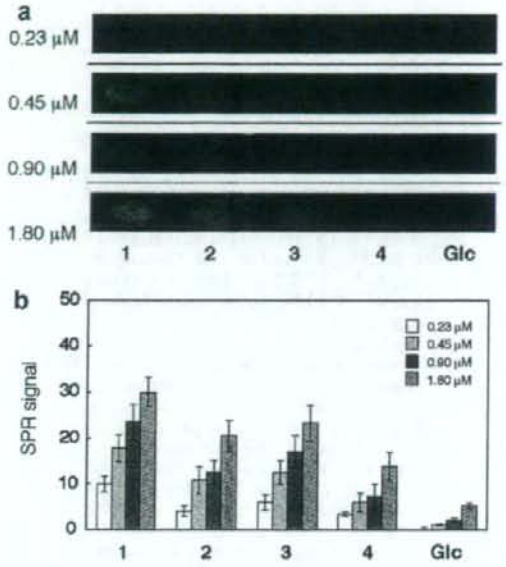

Figure 3. Binding study with rh-vWf-A1. (a) SPR difference imaging on the chip immobilized with compounds **1**, **2**, **3**, **4**, and Glcα(1-6)Glc-mono (Glc). Measurements were carried out with analyte in the range between 0.23 and 1.80 μM. (b) Bar graph profiles of different concentrations. The error bars represent +/− SEM.

In conclusion, we have designed new, precisely sulfated oligosaccharides of HP/HS partial structures. These oligosaccharides were efficiently synthesized using appropriate monosaccharide intermediates. Their application in an array type Sugar Chip, using SPR imaging analysis has been shown to be an efficient and specific technology to elucidate the interactions between a protein and multiple sulfated disaccharides, on a real time scale. These techniques can be used for high-throughput screening of protein samples, as well as for solving the structure–function relations of an individual protein–glycosaminoglycan interaction at the molecular and nano-scale.

Acknowledgments

The present work was financially supported by the Preventure program and the Core Research for Evolutional Science and Technology (CREST) of the Japan Science and Technology Agency (JST) to Y.S., and the National Institutes of Health (Grant HL079182) and the Department of Veterans Affairs Research Service to M.S.

Supplementary data

Supplementary data associated with this article can be found, in the online version, at doi:10.1016/j.bmcl.2008.01.069.

References and notes

1. For reviews, see: (a) Love, K. R.; Seeberger, P. H. *Angew. Chem. Int. Ed.* **2002**, *41*, 3583; (b) Feizi, T.; Fazio, F.; Chai, W.; Wong, C. H. *Curr. Opin. Struct. Biol.* **2003**, *13*, 637; (c) Wang, D. *Proteomics* **2003**, *3*, 2167; (d) Shin, I.; Park, S.; Lee, M. *Chem. Eur. J.* **2005**, *11*, 2894; (e) Ortiz Mellet, C.; Garcia Fernandez, J. M. *ChemBioChem* **2002**, *3*, 819.
2. For articles, see: (a) Blixt, O.; Head, S.; Mandala, T.; Scanlan, C.; Hufflejt, M. E.; Alvarez, R.; Bryan, M. C.; Fazio, F.; Calarese, D.; Stevens, J.; Razi, N.; Stevens, D. J.; Skehel, J. J.; van Die, I.; Burton, D. R.; Wilson, I. A.; Cummings, R.; Bovin, N.; Wong, C. H. *Proc. Natl. Acad. Sci. U.S.A.* **2004**, *101*, 17033; (b) Chevolet, Y.; Martins, J.; Milosevic, N.; Léonard, D.; Zeng, S.; Malissard, M.; Berger, E. G.; Maier, P.; Mathieu, H. J.; Crout, D. H. G.; Sigrist, H. *Bioorg. Med. Chem.* **2001**, *9*, 2943; (c) Park, S.; Lee, M. R.; Pyo, S. J.; Shin, I. *J. Am. Chem. Soc.* **2004**, *126*, 4812; (d) Burn, M. A.; Disney, M. D.; Seeberger, H. P. *ChemBioChem* **2006**, *7*, 421; (e) Houseman, B. T.; Mrksich, M. *Chem. Biol.* **2002**, *9*, 443; (f) Fazio, F.; Bryan, M. C.; Blixt, O.; Paulson, J. C.; Wong, C. H. *J. Am. Chem. Soc.* **2002**, *124*, 14397; (g) Lee, M.; Shin, I. *Angew. Chem. Int. Ed.* **2005**, *44*, 2881; (h) Schwarz, M.; Spector, L.; Gargir, A.; Shtevi, A.; Gortler, M.; Altstock, R. T.; Dukler, A. A.; Dotan, N. *Glycobiology* **2003**, *13*, 749; (i) Zhou, X. C.; Zhou, J. H. *Biosens. Bioelectron.* **2006**, *21*, 1451; (j) Manimala, J. C.; Roach, T. A.; Li, Z. T.; Gildersleeve, J. C. *Angew. Chem. Int. Ed.* **2006**, *45*, 3607; (k) Wang, D.; Liu, S.; Trummer, B. J.; Deng, C. *Nat. Biotechnol.* **2002**, *20*, 275; (l) Chevolet, Y.; Bouillon, C.; Vidal, S.; Morvan, F.; Meyer, A.; Cloarec, J. J.; Jochum, A.; Parly, J. P.; Vasseur, J. J.; Souteyrand, E. *Angew. Chem. Int. Ed.* **2007**, *46*, 2398.
3. Recent carbohydrate chips immobilized sulfated oligosaccharide, see: (a) Suda, Y.; Arano, A.; Fukui, Y.; Koshida, S.; Wakao, M.; Nishimura, T.; Kusumoto, S.; Sobel, M. *Bioconjugate Chem.* **2006**, *17*, 1125; (b) de Paz, J. L.; Noti, C.; Seeberger, P. H. *J. Am. Chem. Soc.* **2006**, *128*, 2766; (c) de Paz, J. L.; Spillmann, D.; Seeberger, P. H. *Chem. Commun.* **2006**, 3116; (d) Noti, C.; de Paz, J. L.; Polito, L.; Seeberger, P. H. *Chem. Eur. J.* **2006**, *12*, 8664; (e) Tully, S. E.; Rawat, M.; Hsieh-Wilson, L. C. *J. Am. Chem. Soc.* **2006**, *128*, 7740.
4. (a) Perou, C. M. *Nature* **2000**, *406*, 747; (b) Ramsey, G. *Nat. Biotechnol.* **1998**, *16*, 40; (c) Marshall, A.; Hodgson, J. *Nat. Biotechnol.* **1998**, *16*, 27; (d) DeRisi, J. L.; Lyer, V. R.; Brown, P. O. *Science* **1997**, *278*, 680.
5. (a) Templin, M. F.; Stoll, D.; Schrenk, M.; Traub, P. C.; Vchringer, C. F.; Joos, T. O. *Trends Biotechnol.* **2002**, *20*, 160; (b) Weinberger, S. R.; Dalmasso, E. A.; Fung, E. T. *Curr. Opin. Chem. Biol.* **2002**, *6*, 86; (c) Fung, E. T.; Thulasiraman, V.; Weinberger, S. R.; Dalmasso, E. A. *Curr. Opin. Biotechnol.* **2001**, *12*, 65; (d) Zhu, H. *Science* **2001**, *293*, 2101; (e) MacBeath, G.; Schreiber, S. L. *Science* **2000**, *289*, 1760.
6. (a) Conrad, H. E. *Heparin-Binding Proteins*; Academic Press: San Diego, 1998; (b) Capila, I.; Lindhardt, R. J. *Angew. Chem. Int. Ed.* **2002**, *41*, 390; (c) Turnbull, J.; Powell, A.; Guimond, S. *Trends Cell Biol.* **2001**, *11*, 75; (d) Bernfield, M.; Götte, M.; Park, P. W.; Reizes, O.; Fitzgerald, M. L.; Lincecum, J.; Zako, M. *Annu. Rev. Biochem.* **1999**, *68*, 729; (e) Rabenstein, D. A. *Nat. Prod. Rep.* **2002**, *19*, 312; (f) Casu, B.; Lindahl, U. *Adv. Carbohydr. Chem. Biochem.* **2001**, *57*, 159.
7. For comprehensive review on the synthesis on GAGs, see: Yeung, B. K. S.; Chong, P. Y. C.; Petillo, P. A. *J. Carbohydr. Chem.* **2002**, *21*, 799.

8. Recent articles, see: (a) Lu, L.-D.; Shie, C.-R.; Kulkarni, S. S.; Pan, G.-R.; Lu, X.-A.; Hung, S.-C. *Org. Lett.* **2006**, *8*, 5995; (b) Zhou, Y.; Lin, F.; Chen, J.; Yu, B. *Carbohydr. Res.* **2006**, *341*, 1619; (c) Codée, J. D. C.; Stubba, B.; Schiattarella, M.; Overkleeft, H. S.; van Boeckel, C. A. A.; van Boom, J. H.; van der Marel, G. A. *J. Am. Chem. Soc.* **2005**, *127*, 3767, And references are therein.
9. (a) Suda, Y.; Marques, D.; Kermode, J. C.; Kusumoto, S.; Sobel, M. *Thromb. Res.* **1993**, *69*, 501; (b) Suda, Y.; Bird, K.; Shiyama, T.; Koshida, S.; Marques, D.; Fukase, K.; Sobel, M.; Kusumoto, S. *Tetrahedron Lett.* **1996**, *37*, 1053.
10. Poletti, L. F.; Bird, K. E.; Marques, D.; Harris, R. B.; Suda, Y.; Sobel, M. *Arterioscler. Thromb. Vasc. Biol.* **1997**, *17*, 925.
11. Koshida, S.; Suda, Y.; Fukui, Y.; Ormsby, J.; Sobel, M.; Kusumoto, S. *Tetrahedron Lett.* **1999**, *40*, 5725.
12. Koshida, S.; Suda, Y.; Sobel, M.; Kusumoto, S. *Tetrahedron Lett.* **2001**, *42*, 1289.
13. Spectral data for compound **2**: ^{1}H NMR (600 MHz, D_2O), δ 7.11 (1 H, t, J = 7.9 Hz), 6.77–6.75 (2 H, m), 6.58 (1H, d, J = 7.9 Hz), 5.22 (1H, d, J = 3.4 Hz), 4.97 (1H, brs), 4.14 (1H, brs), 4.05 (1H, brs), 3.92 (1H, brs), 3.82–3.71 (2H, m), 3.70–3.61 (5H, m), 3.59–3.55 (5H, m), 3.38 (3H, s), 3.28 (1H, dd, J = 9.6 and 3.4 Hz), 3.16 (1H, dd, J = 9.6 and 10.3 Hz), 3.09–3.00 (4H, m), 2.34–2.31 (1H, m), 2.27 (2H, t, J = 6.9), 1.87-1.83 (1H, m), 1.63–1.50 (4H, m), 1.37–1.33 (2H, m), ESI-MS (negative mode); Found: *m/z* 484.62 [(M-3Na+H)$^{2-}$], Calcd. for $C_{33}H_{50}N_3O_{22}S_4Na_3$: 1037.15.
14. (a) Davis, N. J.; Flitsch, S. L. *Tetrahedron Lett.* **1993**, *34*, 1181; (b) Anelli, P. L.; Biffi, C.; Montanari, F.; Quici, S. *J. Org. Chem.* **1987**, *52*, 2559.
15. Kovensky, J.; Duchaussoy, P.; Petitou, M.; Sinaÿ, P. *Tetrahedron: Asymmetry* **1996**, *7*, 3119.
16. Spectral data for compound **3**: ^{1}H NMR (600 MHz, D_2O), δ 7.13 (1H, t, J = 8.2 Hz), 7.11 (1H, s), 6.77 (1H, d, J = 8.2 Hz), 6.60 (1H, d, J = 8.2 Hz), 5.44 (1H, d, J = 3.4 Hz), 4.30 (1H, d, J = 7.6 Hz), 4.15 (1H, d, J = 10.3 Hz), 4.01 (1H, d, J = 10.3 Hz), 3.90 (1H, d, J = 11.0 Hz), 3.83–3.82 (1H, m), 3.76–3.71 (3H, m), 3.66–3.60 (6H, m), 3.52 (1H, dd, J = 10.3 Hz, J = 9.6 Hz), 3.42 (3H, s), 3.27–3.18 (3H, m), 3.14 (1H, dd, J = 3.4 Hz, J = 10.3 Hz), 3.07–3.02 (3H, m), 2.34–2.30 (1H, m), 2.30–2.27 (2H, m), 1.88–1.80 (1H, m), 1.65–1.46 (4H, m), 1.35–1.33 (2H, m), ESI-MS (negative mode); Found: *m/z* 484.65 [(M-3Na+H)$^{2-}$], Calcd. for $C_{33}H_{50}N_3O_{22}S_4Na_3$: 1037.15.
17. Spectral data for compound **4**: ^{1}H NMR (600 MHz, D_2O), δ 7.09 (1H, t, J = 7.9 Hz), 7.04 (1H, s), 6.67 (1H, d, J = 7.9 Hz), 6.52 (1H, d, J = 7.9 Hz), 5.43 (1H, d, J = 4.1 Hz), 4.30 (1H, d, J = 8.2 Hz), 3.91 (1H, d, J = 8.9 Hz), 3.83–3.79 (1H, m), 3.79–3.74 (1H, m), 3.70–3.50 (11H, m), 3.38 (3H, s), 3.25–3.18 (2H, m), 3.14 (1H, dd, J = 9.6 and 9.6Hz), 3.11–2.96 (4H, m), 2.35–2.28 (1H, m), 2.26 (2H, t, J = 6.9 Hz), 1.86–1.80 (1H, m), 1.65–1.45 (4H, m), 1.45–1.27 (2H, m), ESI-MS (negative mode); Found: *m/z* 444.71 [(M-2Na)$^{2-}$], Calcd. for $C_{33}H_{51}N_3O_{19}S_2Na_2$: 935.21.
18. Binding interactions were measured by use of the SPR imaging sensor, Multi SPRinter (TOYOBO Co. Ltd., Osaka, Japan), under the recommended manufacture's guidelines with slight modification. Array-type Sugar Chips were prepared with the purified ligand-conjugates **1**, **2**, **3**, and **4**. An αGlc-containing ligand-conjugate (Glcα4Glc-mono) was also included in the chips as a non-sulfated control. Typical procedures were as follows. After cleaning the chip surface by UV/O_3 treatment, 1 μl of each sample solution (0.5 mM) in H_2O containing 10% glycerol was spotted on the chip by a spotter (TOYOBO), and left to stand overnight at room temperature. The resulting chip was then washed with water, treated with TEG conjugate[21] to mask the unmodified Au surface, and washed with 0.05% Tween 20 aqueous solution and water in an ultrasonic cleaner. A protein solution in PBS containing 0.05% Tween 20 was injected over the surface at a flow rate of 150 μl/min at various concentrations. The binding interaction was monitored at 25 °C as the change in luminance intensity.
19. Mahalingam, Y.; Gallagher, J. T.; Couchman, J. R. *J. Biol. Chem.* **2007**, *282*, 3221.
20. Cruz, M. A.; Handin, H. I.; Wise, R. J. *J. Biol. Chem.* **1993**, *268*, 21238.
21. TEG conjugate is easily prepared by coupling of thioctic acid and 2-{2-[2-(2-hydroxy-ethoxy)-ethoxy]-ethoxy}-ethylamine.

Glycoconj J (2008) 25:269–278
DOI 10.1007/s10719-007-9102-8

Design and synthesis of versatile ganglioside probes for carbohydrate microarrays

Akihiro Imamura · Takeru Yoshikawa · Tatsuya Komori · Masatoshi Ando · Hiromune Ando · Masahiro Wakao · Yasuo Suda · Hideharu Ishida · Makoto Kiso

Received: 2 November 2007 / Revised: 25 December 2007 / Accepted: 26 December 2007 / Published online: 16 January 2008
© Springer Science + Business Media, LLC 2008

Abstract A series of ganglioside GM1-, GM2-, and GM3-type probes, in which the ceramide portion is replaced with a glucose residue, were systematically synthesized based on a convergent synthetic method.

Keywords Chemical synthesis · Gangliosides · Glycosylation · Carbohydrate probe

Introduction

Gangliosides, anionic glycosphingolipids with various sugar chains containing one or more residues of sialic acid, exist universally on cell surface. They participate in vital processes, such as immune or nervous systems, as molecules responsible for cell–cell and cell–ligand interactions [1, 2]. In particular, a series of gangliosides, such as GM1, GM2 and GM3, are important as regulatory factors for the differentiation of the central nervous system and serve as cell-attachment receptors for some viruses, bacteria and bacterial toxins [3, 4]. Moreover, many profound relationships between those gangliosides and a number of cancers and diseases have been demonstrated [5, 6]. However, the biological functions of gangliosides are not fully understood, due to their structural complexities and the low affinities of interaction with ligands, despite numerous studies conducted to date. To solve these issues, a considerable number of efforts have gone into the development of analytical techniques for sensitive detection of carbohydrate–ligand interactions. Consequently, many carbohydrate microarray technologies have been developed to facilitate glycomics research [7]. Coincidentally, many carbohydrate probes that incorporate specific functional groups such as azide [8], thiol [9] and maleimide [10] have been chemically synthesized for the fabrication of microarrays. Recently, oligosaccharide-immobilized chips (named Sugar_Chips), which provide real-time and high-throughput analysis of oligosaccharide–protein interaction without any labeling of the targeted protein, have been developed [11], in which chemically synthesized oligosaccharides having D-glucose, which provides a reactive aldehyde functionality, at the reducing end were used. The D-glucose residue also serves as a spacer between a targeted sugar chain and a scaffold for immobilization, because of its appropriate hydrophilicity and flexibility. Furthermore, it has been demonstrated that a reducing sugar directly participates in the noncovalent link to a scaffold [12, 13]. Accordingly, as exemplified in Fig. 1, the chemically synthesized oligo-

A. Imamura (✉) · T. Yoshikawa · T. Komori · M. Ando · H. Ishida · M. Kiso (✉)
Department of Applied Bioorganic Chemistry,
Faculty of Applied Biological Sciences, Gifu University,
1-1 Yanagido, Gifu-shi, Gifu 501-1193, Japan
e-mail: gif012@gifu-u.ac.jp
e-mail: kiso@gifu-u.ac.jp

H. Ando
Division of Instrumental Analysis, Life Science Research Center,
Gifu University, 1-1 Yanagido, Gifu-shi,
Gifu 501-1193, Japan

M. Wakao · Y. Suda
Department of Nanostructure and Advanced Materials,
Graduate School of Science and Engineering and Venture
Business Laboratory, Kagoshima University,
Kohrimoto, Kagoshima 890-0065, Japan

M. Kiso
Institute for Integrated Cell-Material Sciences (iCeMS),
Kyoto University,
Kyoto, Japan

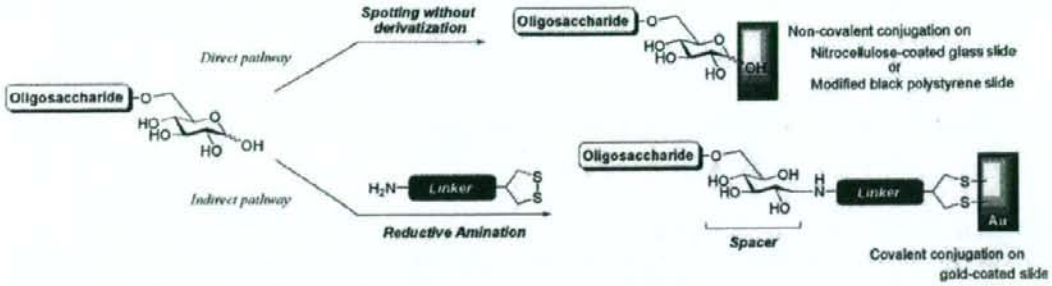

Fig. 1 Two examples for carbohydrate microarray fabrication

saccharide probes are expected to be immobilized by the direct and indirect attachment to scaffolds. We report here the facile synthesis of glucose-ended probes of ganglioside GM1, GM2, and GM3 for carbohydrate microarrays (Fig. 2).

Results and discussion

Taking a look at target molecules, we have hypothetically disconnected them into two parts: common sequence SAα(2→3)Galβ(1→4)Glcβ(1→6)Glc, and the other sugar parts. The common sequence was further disconnected at Galβ(1→4)Glc linkage, providing SAα(2→3)Gal and gentiobiose segments, based on the recently reported efficient syntheses of GM2 analogs [14]. Considering the difficulty to fashion a branch out from galactose residue, the incorporation of GalN parts into Gal residue was planned to be conducted earlier than that of gentiobiose as depicted in Fig. 3.

According to our previous report [14], 2,6-*O*-dibenzylated galactoside was efficiently sialylated at C-3 position with *N*-Troc-protected sialyl donor [15, 16], producing a key sialyl galactoside **4**, which can be obtained in a crystalline form after rough chromatographic purification of the reaction mixture (Fig. 4).

The disaccharide **4** was coupled with Galβ(1→3)GalN **6** [17] or GalN donor **5** in the presence of NIS and TfOH [18] to afford the GM2-core trisaccharide **7** in 97% yield and the GM1-core tetrasaccharide **8** in 89% yield, respectively, as depicted in Table 1.

A series of ganglioside-core frames **4**, **7**, and **8** were converted into the corresponding glycosyl donors **13**, **14**, and **15**, respectively. The selective removal of the Troc group of **4** by the action of zinc–copper couple [19, 20] in acetic acid/1,2-dichloroethane at 40°C proceeded smoothly to give a free amino derivative, which, on successive treatment with acetic anhydride in pyridine afforded the corresponding *N*-acetyl derivative **9**. The use of 1,2-dichloroethane (DCE) was critical for an efficient reduction of Troc group; otherwise the reaction was sluggish. Initially, we were afraid that DCE as solvent itself consumes zinc–copper couple as reductant. Though it is not clear whether DCE is advantageous for electron transfer from zinc–copper couple, we were intriguingly able to observe smooth proceeding of the reaction in a single liquid

Fig. 2 Structure of synthetic ganglioside probes

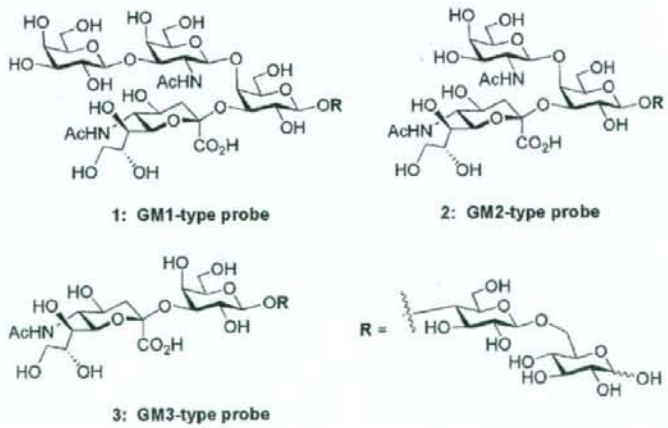

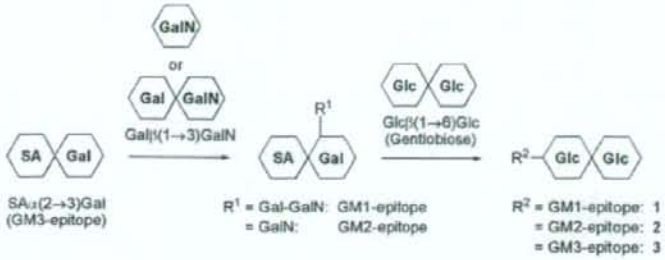

Fig. 3 Systematic reaction scheme for preparation of the reductive glucose-functionalized ganglioside probes

phase within a short time. The cleavage of benzyl groups was executed by hydrogenolysis and the following benzoylation of the resulting hydroxyl groups gave **11**. Libration of the anomeric hydroxyl group of **11** was achieved by treatment with ceric ammonium nitrate (CAN) in acetonitrile–toluene–water (6:5:3) [21]. The obtained hemiacetal was then converted into the β-trichloroacetimidate **13**, which was ready for the final glycosylation with the gentiobiose acceptor **21** as mentioned hereinafter. Interestingly, the use of less than a stoichiometric amount of DBU resulted in the predominant formation of the β-imidate derivative. The conversion of **7** and **8** into the corresponding donor **14** and **15** were also achieved by similar procedure, respectively. (Scheme 1)

Scheme 2 shows the preparation of the gentiobiose acceptor **21** as the common synthetic block, which was expected to have an enhanced reactivity at C-4 hydroxyl due to the effect of electron-donating benzyl groups. Coupling of the known glucose donor **16** [22] and acceptor **17** [23] was conducted in the presence of NIS and TfOH in CH_2Cl_2 at 0°C to give the disaccharide **18** in 90% yield. The β-configuration of the newly formed intersaccharide linkage between **16** and **17** is apparent from the relatively large coupling constant (8.2 Hz) between H-1′ and H-2′ in ^{1}H NMR spectra. Removal of the benzoyl groups under conventional conditions and benzylation of the hydroxyl groups gave **20** with a yield of 88% in two steps. Finally, reductive opening of the benzylidene group was achieved by a treatment with triethylsilane and $BF_3{\cdot}OEt_2$ in CH_2Cl_2 [24] to afford **21** with a yield of 85%.

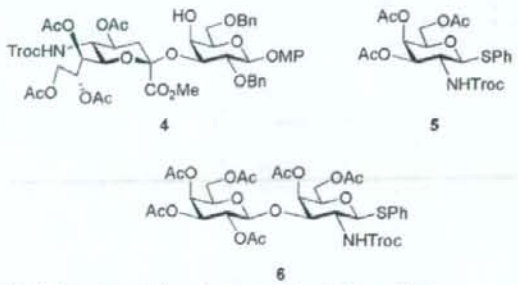

Fig. 4 Structure of glycosyl acceptor (**4**) and donors (**5**, **6**)

Scheme 3 incorporates final glycosylations of **21** with a series of ganglioside-core donors, **13**, **14**, and **15** in the presence of TMSOTf in CH_2Cl_2 at 0°C. The β-imidate **13** was coupled with the gentiobiose acceptor **21** by treatment with TMSOTf at 0°C to afford the desired β-glycoside **22** in an excellent yield. The α-imidate **14** and **15** were subjected to the glycosidation with **21** under essentially the same conditions for **13** to give **23** and **24** in good yields, respectively. Finally, global deprotection of the above-mentioned glycans was conducted. After de-acylation under Zemplén conditions and subsequent saponification of the fully protected oligosaccharides, **24**, **23**, and **22**, hydrogenolysis for each resultant compound was performed in the presence of $Pd(OH)_2/C$ under H_2 atmosphere to afford the target carbohydrate probes **1**, **2** and **3** in good to excellent yields, respectively.

In conclusion, we have succeeded in the synthesis of ganglioside GM1-, GM2-, and GM3-type probes for carbohydrate microarray analyses. It was found that the convergent synthetic strategy between the defined ganglioside-core frame and the reducing end glucose can be used for the synthesis of complex ganglioside probes. In addition, synthesized ganglioside probes are currently used as one of the oligosaccharide probes on immobilized-chips by Suda's group. We are currently underway to expand the existing pool of functional carbohydrate probes containing more complex gangliosides.

Experimental

General procedures

All reactions were carried out under a positive pressure of argon, unless otherwise noted. All chemicals were purchased from commercial suppliers and used without further purification, unless otherwise noted. Molecular sieves were purchased from Wako Chemicals Inc. and dried at 300°C for 2 h in muffle furnace prior to use. ^{1}H NMR and ^{13}C NMR spectra were recorded with a Varian Inova 400/500 spectrometer and a JEOL ECA 500/600 spectrometer. Chemical shifts are reported in parts per million (ppm) downfield from tetramethylsilane. Data are presented as

Table 1 Glycosylation of 4 with glycosyl donors **5** and **6**

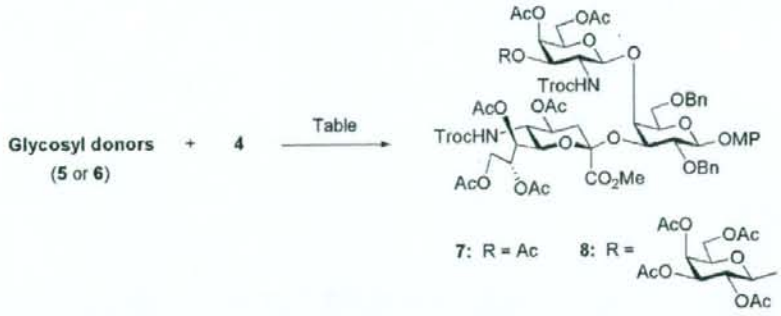

Entry	Donor	Condition	Temp.[°C]	Product	% Yield
1	**5**	NIS TfOH MS4Å CH_2Cl_2	0	**7**	97
2	**6**		-40	**8**	89

follows: Chemical shift, multiplicity (s=singlet, d=doublet, t=triplet, dd=double of doublet, m=multiplet and/or multiple resonances), integration, coupling constant in Hertz (Hz). MALDI-TOF MS spectra were recorded in the positive ion mode on a Bruker Autoflex with the use of α-cyano-4-hydroxy-cinnamic acid (CHCA) as a matrix. Optical rotations were measured with a 'Horiba SEPA-300' polarimeter. Column chromatography was performed on silica gel (Fuji Silysia Co., 80 and 300 mesh). Reactions were monitored by TLC on silica gel $60F_{254}$ (Merck, glass plate) and the compounds were detected by examination under UV light (2,536 Å) and visualized by dipping the plates in a 10% sulfuric acid–ethanol solution or 20% phosphomolybdic acid–ethanol solution followed by heating. Organic solutions were concentrated by rotary evaporation below 45°C under reduced pressure. Solvent systems in chromatography were specified in *v/v*.

4-Methoxyphenyl {methyl 5-acetamido-4,7,8,9-tetra-O-acetyl-3,5-dideoxy-D-glycero-α-D-galacto-2-nonulopyranosylonate-(2→3)}-4-O-acetyl-2,6-di-O-benzyl-β-D-galactopyranoside (**9**) To a solution of compound **4** (500 mg, 465 μmol) in 1,2-dichloroethane (6.1 ml) were added acetic acid (18.3 ml) and zinc–copper couple (2.50 g). The mixture was stirred for 1.5 h at 40°C, as the proceeding of the reaction was monitored by TLC ($CHCl_3$/MeOH=15:1). The

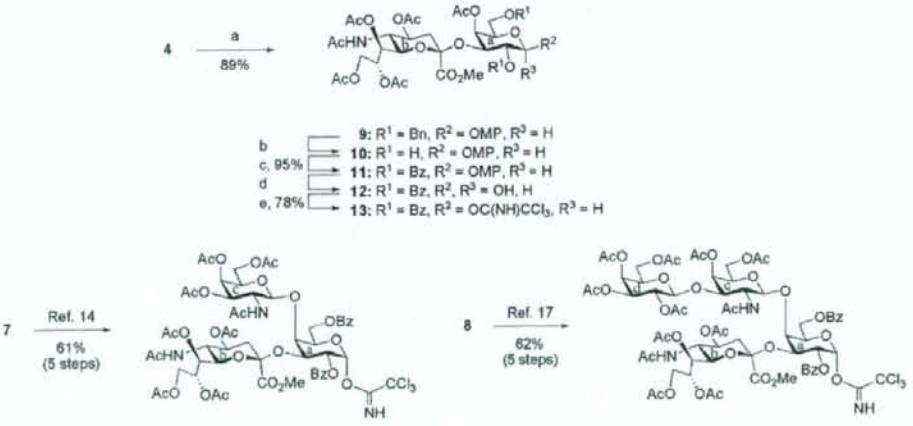

Scheme 1 Conversion of ganglioside-core frames to the corresponding glycosyl donors. Reagents and conditions: *a* Zn-Cu, AcOH, 1,2-DCE, 40°C then Ac_2O, Py; *b* $Pd(OH)_2$/C, H_2, EtOH; *c* Bz_2O, Py; *d* CAN, CH_3CN-PhMe-H_2O (6/5/3); *e* CCl_3CN, DBU, CH_2Cl_2, 0°C

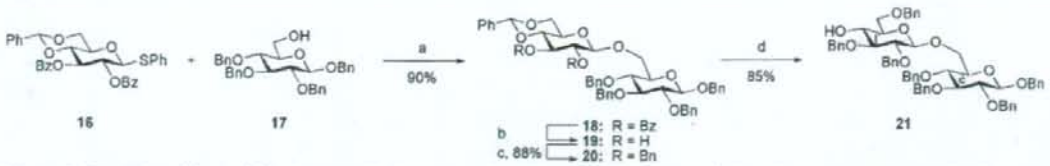

Scheme 2 Preparation of the gentiobiosyl acceptor **21**. Reagents and conditions: *a* NIS, TfOH, MS4Å, CH_2Cl_2, 0°C; *b* NaOMe, MeOH-THF (2/1); *c* BnBr, NaH, DMF; *d* TESH, $BF_3{\cdot}OEt_2$, CH_2Cl_2

reaction mixture was filtered through Celite. The combined filtrate and washings was extracted with $CHCl_3$, and the organic layer was washed with H_2O, sat. Na_2CO_3, and brine, dried over Na_2SO_4 and concentrated. To a solution of the residue in pyridine (5.0 ml) was added acetic anhydride (2.5 ml). The mixture was stirred for 13 h at ambient temperature, as the proceeding of the reaction was monitored by TLC ($CHCl_3$/MeOH=15:1). The reaction mixture was coevaporated with toluene and extracted with $CHCl_3$. The organic layer was washed with 2 M HCl, H_2O, sat. $NaHCO_3$ and brine, dried over Na_2SO_4 and concentrated. The residue was purified with column chromatography on silica gel (EtOAc/hexane=3:1) to give **9** (406 mg, 89%).; $[\alpha]_D$=−15.4° (*c* 0.9, $CHCl_3$); ^{1}H-NMR (600 MHz, $CDCl_3$): δ 7.45–6.77 (m, 14 H, 2 Ph and 1 MP), 5.53 (m, 1 H, H-8b), 5.33 (dd, 1 H, H-7b), 5.24 (d, 1 H, $J_{5,NH}$=8.9 Hz, NH), 5.07 (m, 2 H, H-1a, 4a), 4.96–4.88 (m, 3 H, H-4b, 2 CH*H*Ph), 4.63 (dd, 1 H, H-3a), 4.53 (d, 1 H, CH*H*Ph), 4.46 (d, 1 H, CH*H*Ph) 4.36 (dd, 1 H, H-9'b), 4.13 (q, 1 H, $J_{5,NH}$= 8.9 Hz, H-5b), 3.96–3.94 (m, 2 H, H-6'a, 9b), 3.85 (s, 3 H, OMe), 3.76–3.73 (m, 5 H, H-2a, 6b, OMe), 3.56–3.52 (m, 2 H, H-5a, 6a), 2.63 (dd, 1 H, H-3b$_{eq}$), 2.12–1.83 (m, 19 H,6 Ac, H-3b$_{ax}$); ^{13}C-NMR (100 MHz, $CDCl_3$) δ 170.9, 170.6, 170.3, 170.2, 170.0, 168.1, 155.1, 151.7, 139.4, 138.0, 128.3, 128.1, 127.7, 127.6, 127.1, 118.2, 114.4, 102.4, 97.1, 78.1, 74.8, 73.5, 73.1, 72.3, 72.2, 69.5, 68.9, 68.7, 68.6, 67.2, 62.2, 55.6, 53.1, 49.2, 37.6, 23.2, 21.3, 20.8, 20.8, 20.5; MALDI MS: *m/z*: calcd for $C_{49}H_{59}O_{20}NNa$: 1,004.35; found: 1,004.35 $[M + Na]^+$.

4-Methoxyphenyl {methyl 5-acetamido-4,7,8,9-tetra-O-acetyl-3,5-dideoxy-D-glycero-α-D-galacto-2-nonulopyranosylonate-(2→3)}-4-O-acetyl-2,6-di-O-benzoyl-β-D-galactopyranoside **(11)** To a solution of compound **9** (385 mg, 392 μmol) in EtOH (30 ml) was added palladium hydroxide [$Pd(OH)_2$] (20 wt% Pd on carbon; 400 mg). The mixture was vigorously stirred for 4 h at ambient temperature under hydrogen atmosphere, as the proceeding of the reaction was monitored by TLC ($CHCl_3$/MeOH=15:1). The reaction mixture was filtered through Celite. The combined filtrate and washings was concentrated. To a solution of the residue in pyridine (5.0 ml) was added benzoic anhydride (354 mg, 1.57 mmol). The mixture was stirred for 16 h at ambient temperature, as the proceeding of the reaction was monitored by TLC ($CHCl_3$/MeOH=15:1). The reaction mixture was coevaporated with toluene and extracted with $CHCl_3$. The organic layer was washed with 2 M HCl, H_2O, sat. $NaHCO_3$ and brine, dried over Na_2SO_4 and concentrated. The residue was purified with column chromatography on silica gel (EtOAc/hexane=3:1) to give **11** (380 mg, 95%); $[\alpha]_D$=+ 27.9° (*c* 4.2, $CHCl_3$); ^{1}H-NMR (600 MHz, $CDCl_3$): δ 8.17–6.67 (m, 14 H, 2 Ph and 1 MP), 5.59 (m, 1 H, H-8b), 5.55 (t, 1 H, $J_{1,2}$=8.3 Hz, $J_{2,3}$=10.3 Hz, H-2a), 5.26 (d, 1 H, $J_{1,2}$=8.3 Hz, H-1a), 5.20 (dd, 1 H, $J_{6,7}$=2.8 Hz, H-7b), 5.16 (d, 1 H, $J_{3,4}$=3.4 Hz, H-4a), 5.14 (d, 1 H, NH), 4.87 (dd, 1 H, $J_{2,3}$=10.3 Hz, $J_{3,4}$=3.4 Hz, H-3a), 4.85 (m, 1 H, H-4b), 4.46 (t, 1 H, H-6'a), 4.35 (dd, 1 H, H-6a), 4.27 (dd, 1 H, H-9'b), 4.19 (t, 1 H, H-5b), 3.91 (dd, 1 H, H-9b), 3.86–3.79 (m, 4 H, H-5b, OMe) 3.71 (s, 3 H, OMe), 3.61 (dd, 1 H, $J_{6,7}$=2.8 Hz,

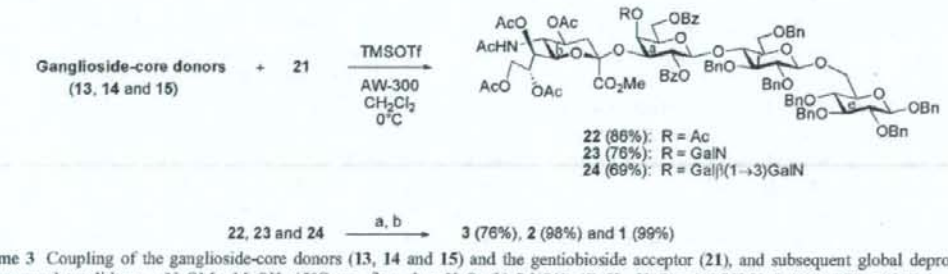

Scheme 3 Coupling of the ganglioside-core donors (**13**, **14** and **15**) and the gentiobioside acceptor (**21**), and subsequent global deprotections. Reagents and conditions: *a* NaOMe, MeOH, 45°C or reflux, then H_2O; (b) $Pd(OH)_2$/C, H_2, H_2O or MeOH-H_2O (5/2), RT or 40°C

H-6b), 2.59 (dd, 1 H, H-3b$_{eq}$), 2.19–1.44 (m, 19 H, 6 Ac, H-3b$_{ax}$); ^{13}C-NMR (100 MHz, $CDCl_3$) δ 170.7, 170.6, 170.3, 170.2, 170.0, 168.0, 165.7, 165.3, 155.4, 151.3, 133.2, 133.0, 130.1, 130.0, 129.7, 128.3, 128.3, 118.9, 114.2, 101.1, 96.7, 71.6, 71.1, 70.8, 69.3, 67.6, 67.4, 66.4, 62.3, 62.0, 55.4, 53.0, 48.7, 37.2, 23.2, 21.3, 20.7, 20.1; MALDI MS: *m/z*: calcd for $C_{49}H_{55}O_{22}NNa$: 1,032.31; found: 1,032.38 $[M + Na]^+$.

{Methyl 5-acetamido-4,7,8,9-tetra-O-acetyl-3,5-dideoxy-D-glycero-α-D-galacto-2-nonulopyranosylonate-(2→3)}-4-O-acetyl-2,6-di-O-benzoyl-β-D-galactopyranosyl Trichloroacetimidate (**13**) To a solution of compound **11** (164 mg, 162 μmol) in mixed solvent (MeCN/PhMe/H_2O= 3.5:2.9:1.7 ml) was added diammonium cerium(IV) nitrate (CAN; 445 mg, 812 μmol). The mixture was stirred for 5 h at ambient temperature, as the proceeding of the reaction was monitored by TLC ($CHCl_3$/MeOH=20:1). The reaction mixture was extracted with $CHCl_3$, and the organic layer was washed with H_2O, sat. $NaHCO_3$ and brine, dried over Na_2SO_4 and concentrated. The residue was purified with column chromatography on silica gel ($CHCl_3$/MeOH= 65:1) to give **12** (147 mg). To a solution of compound 12 in CH_2Cl_2 (5.0 ml) were added trichloroacetonitrile (410 μl, 407 μmol) and 1,8-diazabicyclo[5.4.0]-7-undecene (DBU; 4.9 μl, 33.0 μmol). The mixture was stirred for 2 h at 0°C, as the proceeding of the reaction was monitored by TLC ($CHCl_3$/MeOH=20:1). The reaction mixture was concentrated and the residue was purified with column chromatography on silica gel ($CHCl_3$/MeOH=75:1) to give **13** (132 mg, 78%).; $[\alpha]_D$=+ 18.6° (*c* 0.8, $CHCl_3$); ^{1}H-NMR (600 MHz, $CDCl_3$): δ 8.67 (s, 1 H, C=NH), 8.10–7.41 (m, 10 H, 2 Ph), 6.20 (d, 1 H, $J_{1,2}$=8.3 Hz, H-1a), 5.60–5.56 (m, 2 H, H-2a, H-8b), 5.22–5.20 (m, 2 H, H-4a, H-7b), 4.98 (d, 1 H, $J_{5,NH}$=10.3 Hz, NH-b), 4.93 (dd, 1 H, H-3a), 4.87 (m, 1 H, H-4b), 4.49 (q, 1 H, H-6'a), 4.34–4.29 (m, 3 H, H-5a, 6a, 9'b), 3.93 (dd, 1 H, H-9b), 3.85–3.77 (m, 4 H, H-5b, OMe), 3.60 (dd, 1 H, H-6b), 2.58 (dd, 1 H, H-3b$_{eq}$), 2.19–1.43 (m, 19 H, 6 Ac, H-3b$_{ax}$); ^{13}C-NMR (100 MHz, $CDCl_3$) δ 170.8, 170.7, 170.6, 170.2, 170.2, 170.0, 168.0, 165.7, 165.1, 161.1, 133.2, 130.1, 129.9, 129.7, 129.7, 128.3, 128.3, 96.8, 96.4, 90.3, 77.2, 71.8, 71.5, 71.1, 70.0, 69.4, 67.6, 67.4, 66.5, 62.4, 61.5, 53.1, 48.8, 37.3, 29.7, 23.1, 21.4, 20.8, 20.7, 20.2; MALDI MS: *m/z*: calcd for $C_{44}H_{49}O_{21}N_2Cl_3Na$: 1,069.18; found: 1,069.41 $[M + Na]^+$.

Benzyl 2,3-di-O-benzoyl-4,6-O-benzylidene-β-D-glucopyranosyl-(1→6)-2,3,4-tri-O-benzyl-β-D-glucopyranoside (**18**) To a solution of compound **16** (970 mg, 1.70 mmol) and **17** (762 mg, 1.41 mmol) in CH_2Cl_2 (31 ml) was added molecular sieves 4 Å (1.70 g). The suspension was stirred for 2 h and cooled to 0°C. To the mixture were added *N*-iodosuccinimide (NIS; 765 mg, 3.40 mmol) and trifluoromethanesulfonic acid (TfOH) (30 μl, 0.34 mmol) and stirring was continued for 1.5 h. Completion of the reaction was confirmed by TLC (EtOAc/hexane=1:3). The reaction mixture was filtered through Celite. The combined filtrate and washings was extracted with $CHCl_3$, and the organic layer was washed with sat. Na_2CO_3, sat. $Na_2S_2O_3$ and brine, dried over Na_2SO_4 and concentrated. The residue was purified with column chromatography on silica gel (EtOAc/hexane=1:5) to give **18** (1.26 g, 90%).; $[\alpha]_D$=-9.3° (*c* 1.0, $CHCl_3$); ^{1}H-NMR (600 MHz, $CDCl_3$): δ 7.95–7.13 (m, 35 H, 7 Ph), 5.75 (t, 1 H, $J_{2,3}$=8.8 Hz, $J_{3,4}$=8.6 Hz, H-3f), 5.55 (s, 1 H, >C*H*Ph), 5.52 (t, 1 H, $J_{1,2}$=8.2 Hz, $J_{2,3}$=8.8 Hz, H-2f), 4.91–4.86 (m, 3 H, H-1f, 2 CH*H*Ph), 4.77–4.65 (m, 4 H, 4 CH*H*Ph), 4.49–4.39 (m, 4 H, H-1e, 6f, 2 CH*H*Ph), 4.14 (d, 1 H, J_{gem}= 11.0 Hz, H-6e), 3.99 (t, 1 H, $J_{3,4}$=8.6 Hz, $J_{4,5}$=9.6 Hz, H-4f), 3.89 (br t, 1 H, J_{gem}=10.3 Hz, $J_{5,6}$=9.3 Hz, H-6'f), 3.73–3.63 (m, 2 H, H-6'e, 5f), 3.57 (t, 1 H, $J_{2,3}$=8.4 Hz, H-3e), 3.45–3.40 (m, 3 H, H-2e, 4e, 5e); ^{13}C-NMR (150 MHz, $CDCl_3$) δ 165.7, 165.2, 138.6, 138.5, 138.1, 137.5, 137.0, 133.3, 133.2, 129.9, 129.8, 129.5, 129.3, 129.1, 128.5, 128.4, 128.3, 128.1, 128.0, 127.9, 127.8, 127.7, 127.6, 126.3, 102.5, 101.6, 101.4, 84.7, 82.2, 78.8, 77.8, 75.7, 75.0, 74.9, 74.7, 72.7, 72.3, 71.1, 68.8, 68.4, 67.2, 66.6, 29.8; MALDI MS: *m/z*: calcd for $C_{61}H_{58}O_{13}Na$: 1,021.38; found: 1,021.49 $[M + Na]^+$.

Benzyl 2,3-di-O-benzyl-4,6-O-benzylidene-β-D-glucopyranosyl-(1→6)-2,3,4-tri-O-benzyl-β-D-glucopyranoside (**20**) To a solution of compound **18** (1.25 g, 1.25 mmol) in mixed solvent (MeOH/THF=15:7.5 ml) was added sodium methoxide (28% in MeOH; 24 mg). The mixture was stirred for 7.5 h at ambient temperature, as the proceeding of the reaction was monitored by TLC ($CHCl_3$/MeOH= 50:1). The reaction mixture was neutralized with Dowex (H^+) and filtered through cotton. The combined filtrate and washings was concentrated under diminished pressure. To a solution of the residue in DMF (12.5 ml) were added sodium hydride 60% (200 mg, 5.00 mmol) and benzyl bromide (594 μl, 5.00 mmol). The mixture was stirred for 3 h at ambient temperature, as the proceeding of the reaction was monitored by TLC (toluene/EtOAc= 12:1). Triethylamine and ammonium chloride were added to the reaction mixture. The reaction mixture was washed with H_2O and brine, dried over Na_2SO_4 and concentrated. The residue was purified with column chromatography on silica gel (toluene/EtOAc=40:1) to give **20** (1.07 g, 88%).; $[\alpha]_D$=−21.7° (*c* 1.1, $CHCl_3$); ^{1}H-NMR (600 MHz, $CDCl_3$): δ 7.49–7.21 (m, 35 H, 7 Ph), 5.56 (s, 1 H, >C*H*Ph), 4.96–4.69 (m, 10 H, 10 CH*H*Ph), 4.59 (d, 1 H, $J_{1,2}$=8.2 Hz, H-1f), 4.54–4.45 (m, 3 H, H-1e, 2 CH*H*Ph), 4.33 (dd, 1 H, J_{gem}=9.3 Hz, $J_{5,6}$=4.8 Hz, H-6f), 4.16 (d, 1 H, J_{gem}=11.0 Hz, H-6e), 3.79–3.72 (m, 2 H, H-6'e, 6'f), 3.68–3.64 (m, 3 H, H-2f, 4f, 5f), 3.57 (t, 1 H, $J_{2,3}$=8.5 Hz, $J_{3,4}$=9.0 Hz, H-3e), 3.50–3.47 (m, 2 H, H-2e, 2f), 3.44 (t,

1 H, $J_{3,4}$=9.6 Hz, $J_{4,5}$=9.6 Hz, H-4e), 3.35 (m, 1 H, H-5e); ^{13}C-NMR (150 MHz, $CDCl_3$) δ 138.6, 138.6, 138.8, 138.1, 137.6, 137.5, 129.1, 128.7, 128.5, 128.4, 128.3, 128.3, 128.3, 128.2, 128.1, 128.0, 128.0, 127.9, 127.8, 127.8, 127.7, 127.6, 126.1, 104.3, 102.7, 101.3, 84.8, 82.4, 82.1, 81.6, 81.0, 78.3, 77.3, 75.8, 75.4, 75.2, 75.1, 74.9, 71.3, 68.9, 66.1, 29.8; MALDI MS: *m/z*: calcd for $C_{61}H_{62}O_{11}Na$: 993.42; found: 993.50 $[M + Na]^+$.

Benzyl 2,3,6-tri-O-benzyl-β-D-glucopyranosyl-(1→6)-2,3,4-tri-O-benzyl-β-D-glucopyranoside (**21**) To a solution of compound **20** (82 mg, 84.5 μmol) in CH_2Cl_2 (845 μl) were added triethylsilane (162 μl, 1.01 mmol) and boron trifluoride diethyl etherate ($BF_3{\cdot}OEt_2$; 21.4 μl, 169 μmol). The mixture was stirred for 1.5 h at ambient temperature, as the proceeding of the reaction was monitored by TLC (toluene/EtOAc=12:1). The reaction mixture was diluted with $CHCl_3$ and washed with sat. $NaHCO_3$, H_2O and brine, dried over Na_2SO_4 and concentrated. The residue was purified with column chromatography on silica gel (toluene/EtOAc=20:1) to give **21** (70 mg, 85%).; $[\alpha]_D$=−12.9° (*c* 1.0, $CHCl_3$); ^{1}H-NMR (600 MHz, $CDCl_3$): δ 7.35–7.21 (m, 35 H, 7 Ph), 5.01–4.69 (m, 10 H, 10 CH*H*Ph), 4.59–4.51 (m, 3 H, H-1f, 2 CH*H*Ph), 4.46 (d, 1 H, $J_{1,2}$=9.6 Hz, H-1e), 4.19 (d, 1 H, J_{gem}=11.0 Hz, H-6e), 3.74–3.58 (m, 6 H, H-6'e, 3f, 4f, 5f, 6f, 6'f), 3.50–3.39 (m, 5 H, H-2f, 2e, 3e, 4e, 5e), 2.54 (s, 1 H, -OH); ^{13}C-NMR (150 MHz, $CDCl_3$) δ 138.9, 138.7, 138.5, 138.5, 138.2, 138.0, 137.6, 128.6, 128.5, 128.5, 128.4, 128.3, 128.2, 128.1, 128.0, 128.0, 127.9, 127.8, 127.7, 104.1, 102.7, 84.8, 84.2, 82.4, 81.6, 78.4, 77.3, 75.8, 75.4, 75.3, 75.1, 74.9, 74.8, 74.1, 73.8, 71.8, 71.3, 68.8, 29.8; MALDI MS: *m/z*: calcd for $C_{61}H_{64}O_{11}Na$: 995.43; found: 995.38 $[M + Na]^+$.

Benzyl {methyl 5-acetamido-4,7,8,9-tetra-O-acetyl-3,5-dideoxy-D-glycero-α-D-galacto-2-nonulopyranosylonate-(2→3)}-4-O-acetyl-2,6-di-O-benzoyl-β-D-galactopyranosyl-(1→4)-2,3,6-tri-O-benzyl-β-D-glucopyranosyl-(1→6)-2,3,4-tri-O-benzyl-β-D-glucopyranoside (**22**) To a solution of compound **13** (107 mg, 102 μmol) and **21** (200 mg, 206 μmol) in CH_2Cl_2 (5.0 ml) was added molecular sieves 4 Å (1.00 g). The suspension was stirred for 1 h and cooled to 0°C. To the mixture was added trimethylsilyl trifluoromethanesulfonate (TMSOTf; 3.7 μl, 20 μmol) and stirring was continued for 1 h. Completion of the reaction was confirmed by TLC ($CHCl_3$/MeOH=20:1). The reaction mixture was filtered through Celite. The combined filtrate and washings was extracted with $CHCl_3$, and the organic layer was washed with sat. Na_2CO_3 and brine, dried over Na_2SO_4 and concentrated. The residue was purified with column chromatography on silica gel ($CHCl_3$/MeOH=75:1) to give **22** (170 mg, 86%).; $[\alpha]_D$=+ 2.0° (*c* 0.5, $CHCl_3$); ^{1}H-NMR (500 MHz, $CDCl_3$): δ 8.24–7.15 (m, 45 H, 9 Ph), 5.66 (m, 1 H, H-8b), 5.31 (t, 1 H, $J_{1,2}$=8.0 Hz, $J_{2,3}$= 9.7 Hz, H-2a), 5.18 (dd, 1 H, H-7b), 5.13 (d, 1 H, $J_{1,2}$=8.0 Hz, H-1a), 5.06 (d, 1 H, $J_{3,4}$=3.4 Hz, H-4a), 4.99 (d, 1 H, CH*H*Ph), 4.92–4.66 (m, 12 H, H-3a, 4b, NH, 9 CH*H*Ph), 4.49–4.36 (m, 7 H, H-6'a, 1e, 1f, 4 CH*H*Ph), 4.29 (d, 1 H, H-9'b), 4.13–3.88 (m, 6 H, H-5a, 6a, 5b, 9b, H-6' of Glc units), 3.77 (q, 1 H, H-5b), 3.71 (s, 1 H, OMe), 3.67–3.35 (m, 10 H, H-6b, Glc units), 3.22 (m, 1 H, H-5 of Glc units), 2.52 (dd, 1 H, J_{gem}=12.6 Hz, $J_{3eq,4}$=4.6 Hz H-3b$_{eq}$), 2.13–1.43 (m, 19 H, 6 Ac, H-3b$_{ax}$) ^{13}C-NMR (125 MHz, $CDCl_3$) δ 170.8, 170.7, 170.3, 170.2, 170.1, 168.0, 165.4, 165.1, 139.1, 138.6, 138.4, 138.0, 137.6, 133.3, 133.0, 130.3, 130.0, 129.8, 129.7, 128.6, 128.4, 128.3, 128.3, 128.2, 128.1, 128.1, 127.9, 127.9, 127.7, 127.6, 127.4, 127.3, 127.2, 127.1, 103.7, 102.7, 100.4, 96.9, 84.7, 82.9, 82.3, 81.6, 78.2, 76.3, 75.7, 75.2, 75.1, 74.9, 74.8, 74.8, 74.4, 72.8, 71.7, 71.5, 71.2, 70.4, 69.4, 69.0, 68.5, 67.4, 67.0, 66.5, 62.5, 61.2, 53.0, 48.8, 37.3, 29.7, 23.2, 21.3, 20.8, 20.7, 20.7, 20.3; MALDI MS: *m/z*: calcd for $C_{103}H_{111}O_{31}NNa$: 1,880.70; found: 1,880.96 $[M + Na]^+$.

Benzyl 2-acetamido-3,4,6-tri-O-acetyl-2-deoxy-β-D-galactopyranosyl-(1→4)-{methyl 5-acetamido-4,7,8,9-tetra-O-acetyl-3,5-dideoxy-D-glycero-α-D-galacto-2-nonulopyranosylonate-(2→3)}-2,6-di-O-benzoyl-β-D-galactopyranosyl-(1→4)-2,3,6-tri-O-benzyl-β-D-glucopyranosyl-(1→6)-2,3,4-tri-O-benzyl-β-D-glucopyranoside (**23**) To a solution of compound **14** (58 mg, 43 μmol) and **21** (84 mg, 86 μmol) in CH_2Cl_2 (2.0 ml) was added molecular sieves 4 Å (165 mg). The suspension was stirred for 1 h at ambient temperature and cooled to 0°C. To the mixture was added TMSOTf (1.6 μL, 8.6 μmol) and stirring was continued for 3.5 h. Completion of the reaction was confirmed by TLC ($CHCl_3$/MeOH=15:1). Triethylamine was then added to quench the reaction. The reaction mixture was filtered through Celite. The combined filtrate and washings was extracted with $CHCl_3$, and the organic layer was washed with sat. $NaHCO_3$ and brine, dried over Na_2SO_4 and concentrated. The residue was purified with column chromatography on silica gel ($CHCl_3$/MeOH=50:1) to give **23** (70 mg, 76%).; $[\alpha]_D$=−11.0° (*c* 0.76, $CHCl_3$); ^{1}H-NMR (600 MHz, $CDCl_3$): δ 8.01–7.15 (m, 45 H, 9 Ph), 5.97 (d, 1 H, NH-c), 5.49 (dd, 1 H, $J_{3,4}$=2.7 Hz, H-3c), 5.40 (m, 1 H, H-8b), 5.37 (d, 1 H, $J_{3,4}$=2.7 Hz, H-4c), 5.34 (t, 1 H, $J_{1,2}$= 10.2 Hz, H-2a), 5.25 (d, 1 H, H-7b), 5.14 (br d, 1 H, NH-b), 5.06 (d, 1 H, $J_{1,2}$=8.9 Hz, H-1c), 5.00 (dt, 1 H, $J_{3eq,4}$= 4.8 Hz, H-4b), 4.95–4.88 (m, 4 H, 4 CH*H*Ph), 4.82–4.80 (m, 3 H, 3 CH*H*Ph), 4.79 (d, 1 H, $J_{1,2}$=10.2 Hz, H-1a), 4.72 (t, 2 H, 2 CH*H*Ph), 4.67 (d, 1 H, CH*H*Ph), 4.62 (q, 1 H, H-6c), 4.51 (d, 1 H, CH*H*Ph), 4.47 (d, 1 H, CH*H*Ph), 4.43 (d, 1 H, CH*H*Ph), 4.40 (d, 1 H, $J_{1,2}$=8.2 Hz, H-1f), 4.37 (d, 1 H, $J_{1,2}$= 8.2 Hz, H-1e), 4.28 (d, 1 H, CH*H*Ph), 4.19 (t, 1 H, H-5a), 4.15–3.96 (m, 10 H, H-3a, 4a, 6a, 6'a, 5b, 9b, 9'b, 2c, 6'c, 5e), 3.95 (t, 1 H, H-4f), 3.83–3.81 (m, 4 H, OMe, H-6b), 3.64